

REPORT FROM PILOT ACTION - Report from testing the dynamic model to assess cumulative effect of N(S)WRM

Austria/ WasserCluster Lunz
Pilot catchment Aist

Version 6
January 2020



TABLE OF CONTENT

1.	Introduction.....	1
2.	Application of the hydrological model	2
2.1	Description of the catchment.....	2
2.2	SWAT model description	3
2.3	Watershed delineation.....	4
2.4	Land cover, soils and HRUs definition	6
2.5	Model structure.....	9
2.6	Weather data.....	10
2.7	Point inlet	10
2.8	Ponds and reservoirs	11
2.9	Model calibration and validation for flow at the daily time step.....	11
2.10	Model calibration and validation for flow and sediment at the monthly time step.....	16
3.	Hydraulic modeling.....	22
3.1	Description of the river network.....	22
3.2	Geometric data.....	24
3.3	Description of the model structure	25
3.4	Boundary conditions	25
3.5	Hydrologic and hydraulic data.....	26
3.6	Model calibration and validation	28
3.7	Model uncertainties	29
4.	Hydrological, hydraulic and sediment predictors	30
5.	Siltation model	33
6.	Habitat model.....	35
6.1	Field data	35
6.2	Habitat suitability indices derivation.....	35
6.3	Habitat modeling at the catchment scale	37
6.4	Connectivity assessment	38
6.5	Freshwater Pearl Mussel habitat niche.....	38
7.	Baseline conditions.....	40
7.1	Siltation status.....	41
7.2	Habitat status	42
7.3	Connectivity.....	43
7.4	Siltation effects on habitat availability.....	44

7.5	Baseline summary	45
8.	NSWRMs testing in the Aist catchment	46
8.1	Methodology	46
8.2	Effects on hydrology and sediment generation	48
8.3	Effects on hydraulics.....	50
8.4	Effects on sand accumulation	51
8.5	Effect on habitat availability.....	52
8.6	NSWRMs testing conclusions	54
9.	Conclusions.....	55
10.	References.....	56
11.	Appendix A – SWAT Data source.....	59
12.	Appendix B– SWAT calibration results	61



1. INTRODUCTION

A suite of dynamic models was implemented in the Aist catchment in order to link catchment scaled hydrology, reach hydraulics, sand accumulation and habitat availability. This sequence of interlinked models is usually referred in the scientific literature as **ecohydrological modeling cascade (EMC)**.

The developed ecohydrological modeling cascade (Fig. 1) is composed of a sequence of models structured in a way that the outputs from the coarser spatial scale can be used as inputs to the finer model (Kiesel et al., 2010).

The implemented EMC is composed of:

- the ecohydrological Soil and Water Assessment Tool 2012 (SWAT, Arnold et al., 2012) for discharge and sediment generation, and transport at the catchment scale,
- the one-dimensional hydraulic model Hydraulic Engineering Center – River Analysis System (HEC-RAS) 5.0.5 (USACE 2015) for reach scale hydraulics,
- a Random Forest (RF) as provided by the package ‘caret’ in R (Kuhn 2009; R Development Core Team, 2019) for fine sediment accumulation, and
- species distribution models (SDMs) for the target species Freshwater Pearl Mussle (FPM) as provided in the package biomod2 in R (Thuiller et al., 2013).

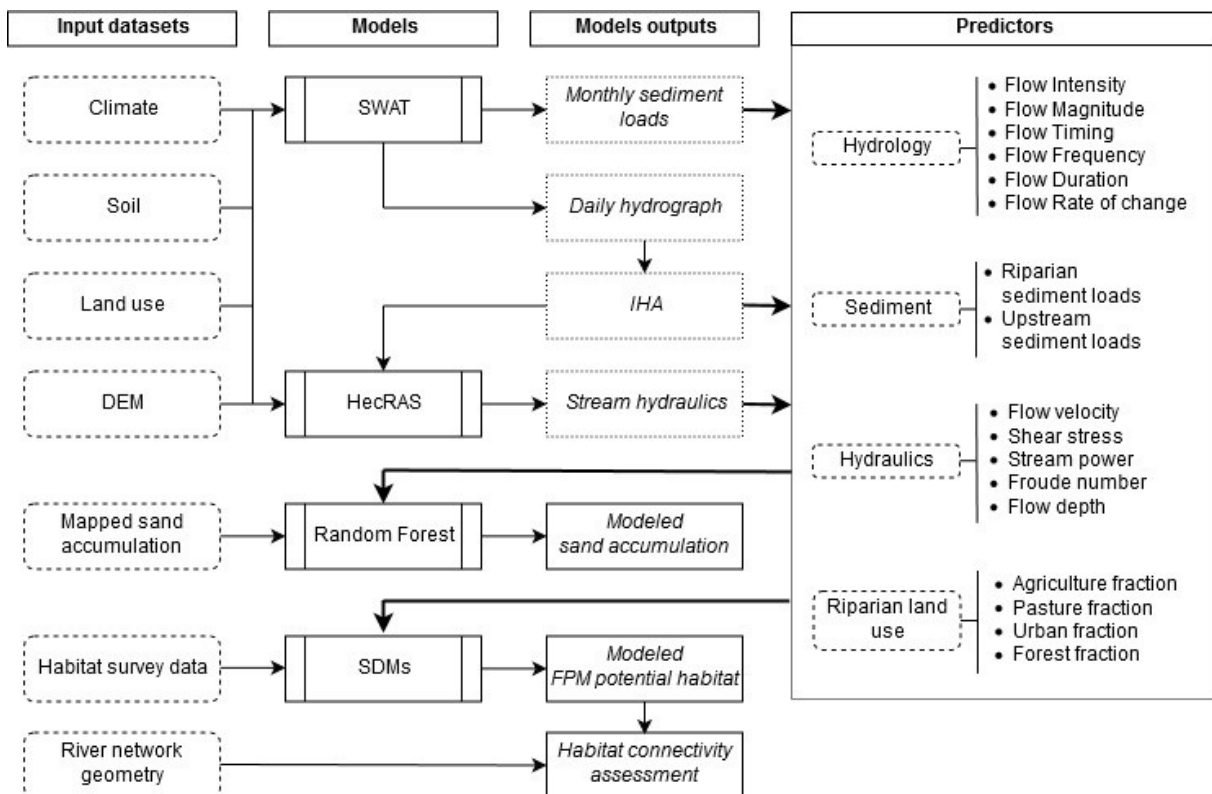


Figure 1 – Scheme describing the implementation of dynamic models (ecohydrological modeling cascade) for the Aist pilot catchment

Note: in this report the terms siltation, fines accumulation and sand accumulations are used as synonyms and refer to accumulations of sediments with a mean diameter between 1 and 10 mm that are resulting from the erosion of the granitic substrate. Refer to Hauer et al., 2015; Leitner et al., 2015; Scheder et al., 2015 for further details on the siltation issue in the region.



2. APPLICATION OF THE HYDROLOGICAL MODEL

The hydrological model SWAT (Soil and Water Assessment Tool, Arnold et al., 2012) was implemented for the Austrian pilot catchment Aist. The working steps for the implementation of the model were:

1. Input data preprocessing
2. Model setup
3. Model calibration and validation for flow
4. Model calibration and validation for sediments

2.1 Description of the catchment

The Aist Basin was chosen as a pilot catchment in Austria because the existing topographical characteristics as well as the prevailing problems, pressures and water management measures make it an appropriate case study region for a NSWRM approach. It is a representative catchment for the Austrian part of the ecoregion Central Uplands (low mountain ranges with plateaus and gorges), a region that geologically belongs to the Bohemian Massif (Variscan orogeny, 370-290 mil. years) with the prevailing bedrocks granite and gneiss. Within this region all river catchments share one common problem: siltation from granite weathering and erosion, causing ecological problems in rivers (habitat degradation) as well as problems for water and flood management (riverbed rising). Further issues in the Aist catchment are: (a) hydromorphological deficits due to river regulations and flood protection measures, and (b) poor ecological status in several river stretches (assessment for WFD, Austrian Water Management Plan). NSWRM can help mitigate the existing problems in the catchment and improve conditions related to the aspects of water quality, sediment balance, nutrient cycle and habitat diversity.

Table 1 – Characteristics of the Aist pilot catchment.

*Note: * From multiannual statistic 1984-2016; ** From multiannual statistic 1981-2010; *** From CORINE LandCover 2012*

Characteristic	Unit	Value
<i>Character of catchment</i>		<i>Central Uplands</i>
<i>Catchment size:</i>	<i>km²</i>	<i>647</i>
<i>Average flow low/avg/high*</i>	<i>m³/s</i>	<i>5.1/6.4/7.8</i>
<i>Extreme flow low/high*</i>	<i>m³/s</i>	<i>0.44/336.6</i>
<i>Annual precipitation low/avg/high**</i>	<i>mm</i>	<i>726/835/993</i>
<i>Annual air temperature min/avg/max**</i>	<i>°C</i>	<i>5.4/7.1/9.5</i>
<i>Agriculture area***</i>	<i>%</i>	<i>48.9</i>
<i>Urban area***</i>	<i>%</i>	<i>3.9</i>
<i>Forest area***</i>	<i>%</i>	<i>46.8</i>
<i>Open Water area***</i>	<i>%</i>	<i>0.01</i>
<i>Flooded area (1/100 years)</i>	<i>km²</i>	<i>1.9</i>
<i>Artificial drainage area</i>	<i>km²</i>	<i>0</i>

The main tributaries in the Aist catchment are the Feldaist, draining the northwestern area, and the Waldaist, draining the northeastern area. After the confluence of Feldaist and Waldaist at the municipality Hohensteg, the Aist has 14 more kilometers until it joins the Danube south of Schwertberg.

In the Waldaist area forestry and extensive pastures are dominating, whereas the Feldaist area is dominated by more intensive agricultural practices. There is a north to south and an east to west gradient regarding land use intensity and population density (Fig. 2; Table 1).

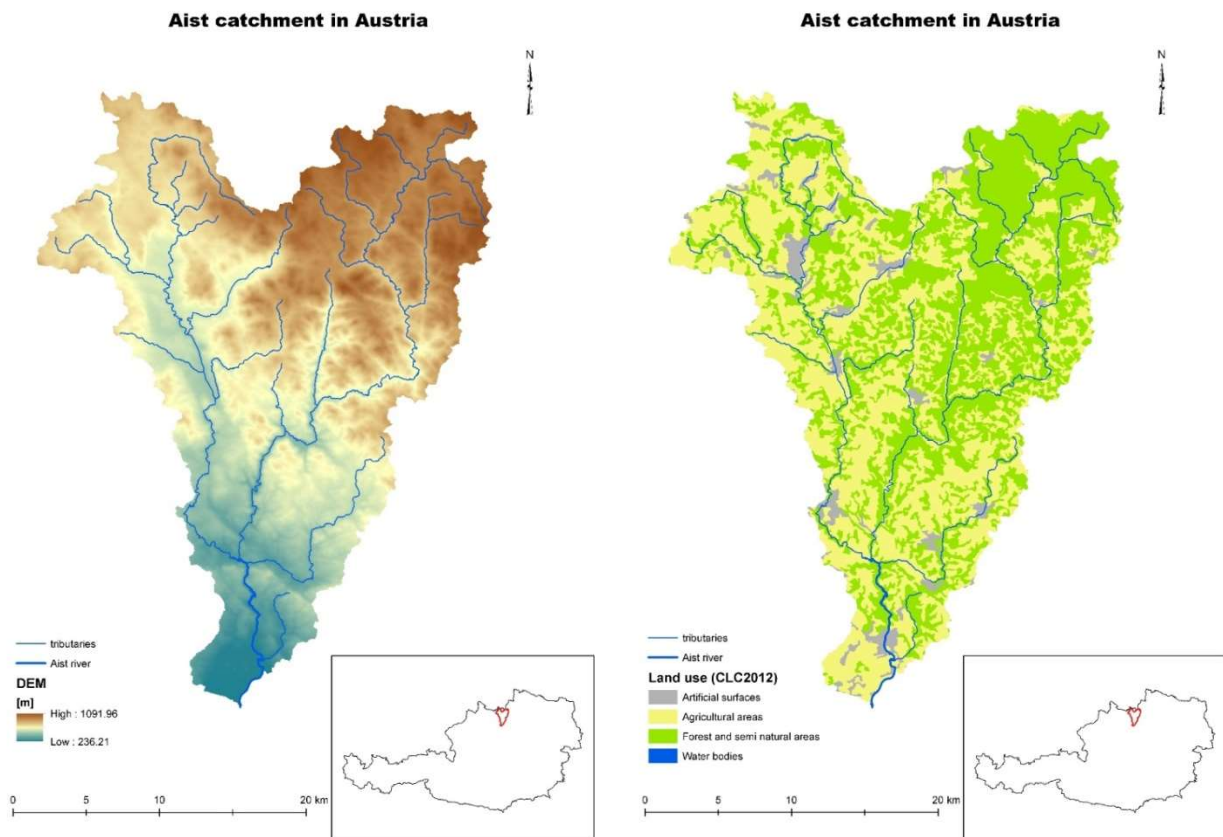


Figure 2 – Aist catchment hydrography, orography (left) and land use (right)

2.2 SWAT model description

The hydrological aspect was modeled using the Soil and Water Assessment Tool (SWAT), a semi-distributed process-based hydrological model (Fig. 3, Arnold et al., 2012). SWAT implements subroutines to compute the hydrological balance, sediment balance, crop growth, water, sediments, and nutrient routing in the stream network (for detailed description of processes and flows modeled, refer to: Gassman et al., 2007). The time step for the simulation can be daily, monthly or annual.

The hydrologic module can simulate several physical-based processes, among others: surface and subsurface runoff (shallow and deep aquifers), evapotranspiration, snowmelt and retention in reservoirs. The sediment module simulates sediments generation in the catchment (through the modified universal soil loss equation, MUSLE) and transport by the river (deposition, erosion, resuspension).

The simulated catchment is subdivided in hydrological response units (HRU), that are portions of the landscape with uniform characteristics (regarding land use, slope, soil properties), thus allowing to increase the computational efficiency by reducing the spatial complexity of the model. Hydrological, sediments and chemicals mass balances are computed for each HRU separately, averaged at the subcatchment level and routed in the stream network.

Inputs to the model are:

- topographic, land use, soil type maps;
- climatic data: daily precipitation, maximum and minimum air temperature;
- Agricultural practices: tillage, irrigation, fertilization, planting and harvesting schedules;
- Landscape features: ponds, wetlands, reservoirs data;
- External point inlets;
- Water, sediment, nutrient point sources;
- Water flows and sediment loads time series.

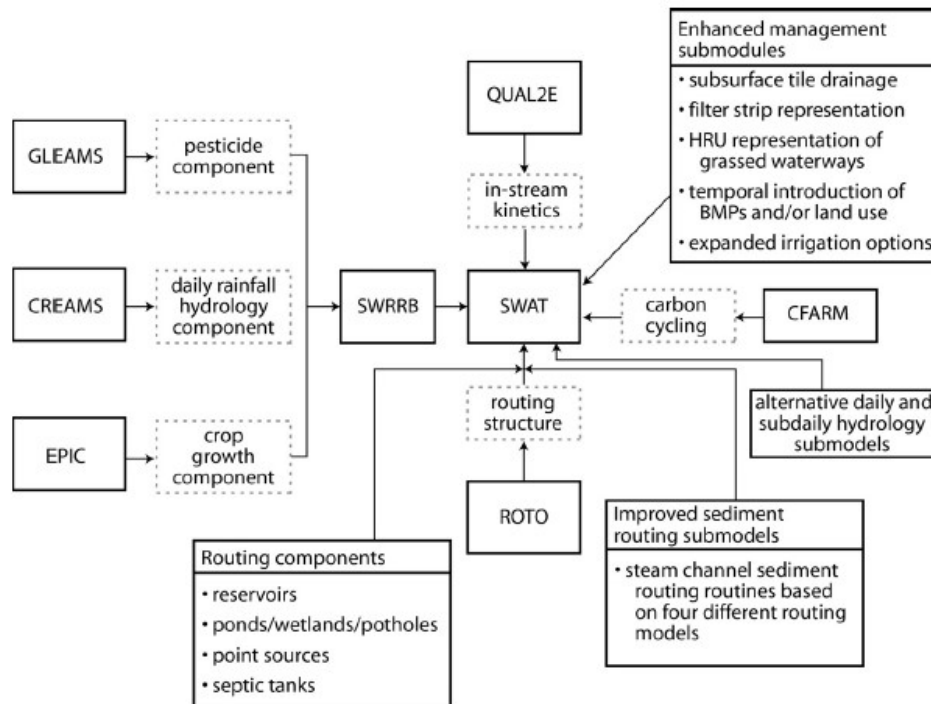


Figure 3 – SWAT model structure, from Arnold et al., 2012

Calibration and validation of the model were performed using discharges and sediment loads time series via a dedicated standalone optimization (SWAT-CUP) program that allows also for sensitivity and uncertainty analysis.

SWAT is a powerful tool for scenario analysis depicting different management practices. For this reason, SWAT has been widely used for BMPs and management practices simulation and effectiveness evaluation at the catchment scale (Waidler et al., 2011).

The software used in the Hydrologic dynamic modeling:

- arcSWAT, an ArcGIS interface has been used for the model setup, (Winchell et al., 2007);
- SWAT model version v664 (<https://swat.tamu.edu/>);
- SWAT-CUP, a standalone program for calibration, sensitivity and uncertainty analysis (Abbaspour, 2013)
- Results were processed and analyzed using R studio (<https://www.r-project.org/>).

2.3 Watershed delineation

The watershed delineation step is needed to define the geometrical and morphological features of the watershed starting from a digital elevation model (DEM). The watershed was delineated

using the dedicated tool in the arcSWAT interface. A DEM with a resolution of 10m was used in this step (Fig. 4). Due to the lack of a proper DEM in the northeastern part of the catchment, it was not possible to define a river network there. Therefore, the modeled part of the catchment is slightly smaller than its actual area. Nevertheless, the hydrological response was computed by assuming a uniform precipitation and a linear response of the catchment to rain in the unmodeled part.

A threshold on the cumulated area of 50 ha was imposed to define which cell is to be considered a river and which not using a common approach in hydrology. The river network obtained this way (Fig. 4) is not showing deviations from the river network from official national layers.

Based on the obtained river network, the watershed was split into 103 sub-basins (Fig. 5).

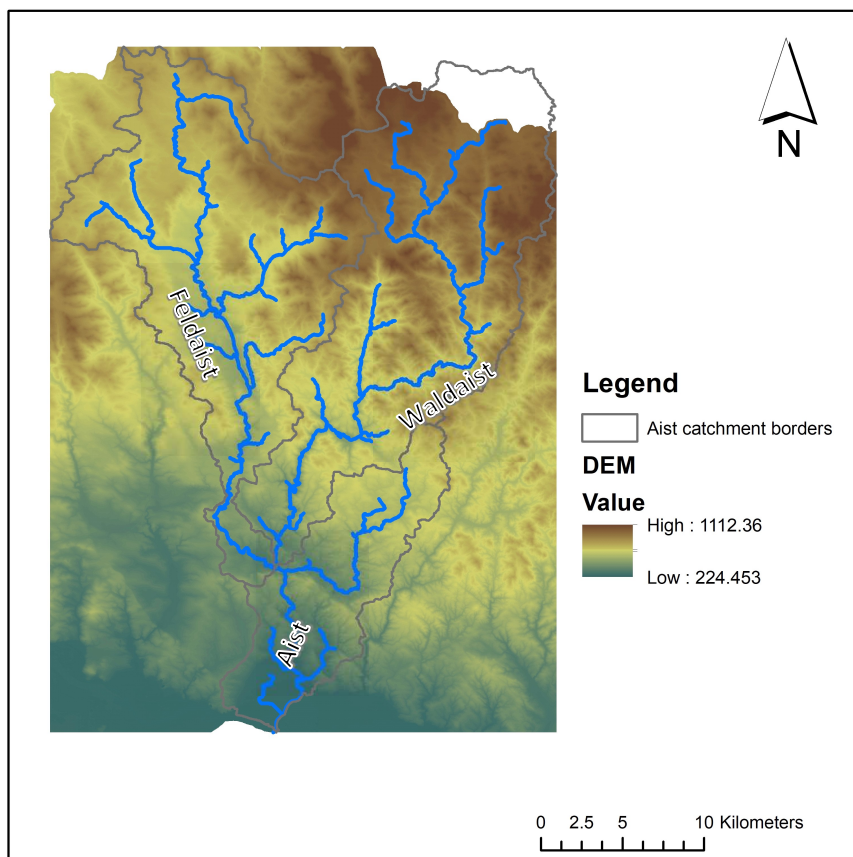


Figure 4 – Input DEM for the watershed delineation and river network obtained from the watershed delineation process

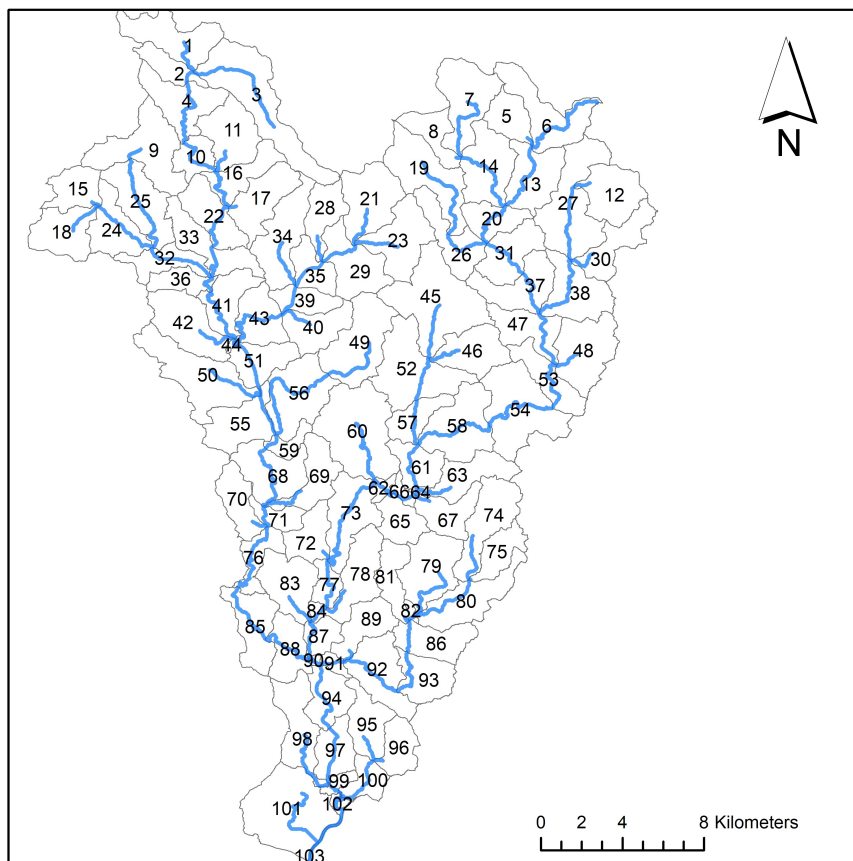


Figure 5 – Subcatchments subdivision of the delineated watershed

2.4 Land cover, soils and HRUs definition

The HRU definition process is based on the overlay of land use, soil and slope maps to identify patches in the landscape having a uniform hydrological response. Since the slope map can be easily obtained from a DEM, the input data needed by this process are a land use map and a soil map. Since usable land use and soil products are not available from local, national or federal Austrian databases, some preprocessing was needed.

The land use map was obtained by merging the federal agricultural INVEKOS dataset that contains information on the crops at the field level and the European CORINE map that provides rough information (Table 2). The CORINE land use agricultural polygons have been replaced with data from INVEKOS dataset, leading to a land use map with an accurate spatial representation of agricultural land uses (Fig. 6).

Table 2 – INVEKOS and CORINE land use maps informations

	INVEKOS	CORINE
Resolution	Field scale	25 ha / 100 m
Limitation	Only agricultural land use, no informations on other land uses	Poor definition of agricultural land use; polygons sometimes inaccurate
Source	https://www.data.gv.at/katalog/dataset	https://land.copernicus.eu/pan-european/corine-land-cover

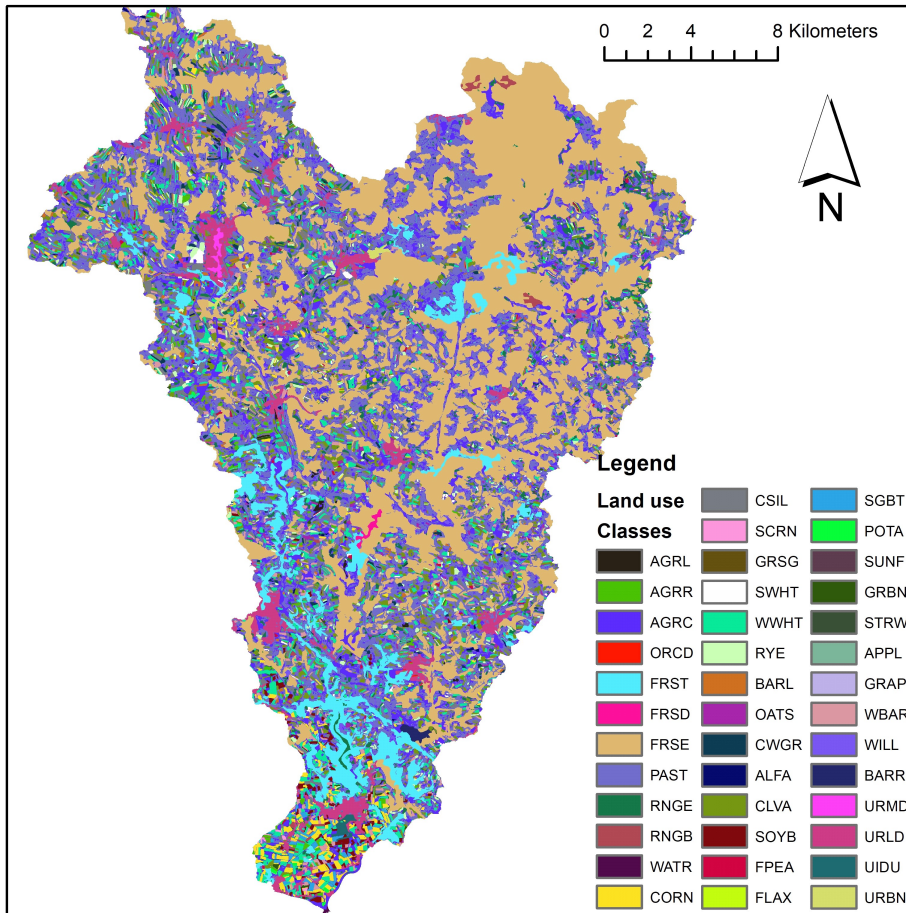


Figure 6 – Land use map resulting from CORINE and INVEKOS integration

A lookup table was used to convert the local land use definitions to SWAT land use and crop classes. For major crops it was possible to identify a 1 to 1 relationship between INVEKOS classes and SWAT classes (winter wheat = WWHT, soybean = SOYB, corn = CORN, corn silage = CSIL, winter barley = WBARL, pasture = PAST). Some minor crops (less than 2% of the catchment area) were aggregated into classes AGRR and AGRL (generic agricultural classes). The generic land use AGRC was assigned to the agricultural part of CORINE map not covered by INVEKOS and then further split (land use split function in the HRU definition process) keeping the same major crop shares resulting from INVEKOS map.

The soil map was obtained by processing of a map of a global dataset, SoilGrids (<https://soilgrids.org/>), a global raster with a resolution of 250 m.

Homogeneous soil patches were identified using the k-means clusterization algorithm in the R computing environment. Inputs for the algorithm were Soilgrids textural (Sand, Silt, Clay percentages) and organic matter content rasters from the SoilGrids database for three soil depths: 0-5; 5-30, 30-200 cm. The algorithm provided clusters of raster cells minimizing the intra-class variance and maximizing the inter-classes variance. 10 soil classes were generated (Fig. 7).

Pedotransfer functions (Saxton, 2006) were used to obtain the parameters that SoilGrid database is not providing: soil albedo, saturated hydraulic conductivity, bulk density.

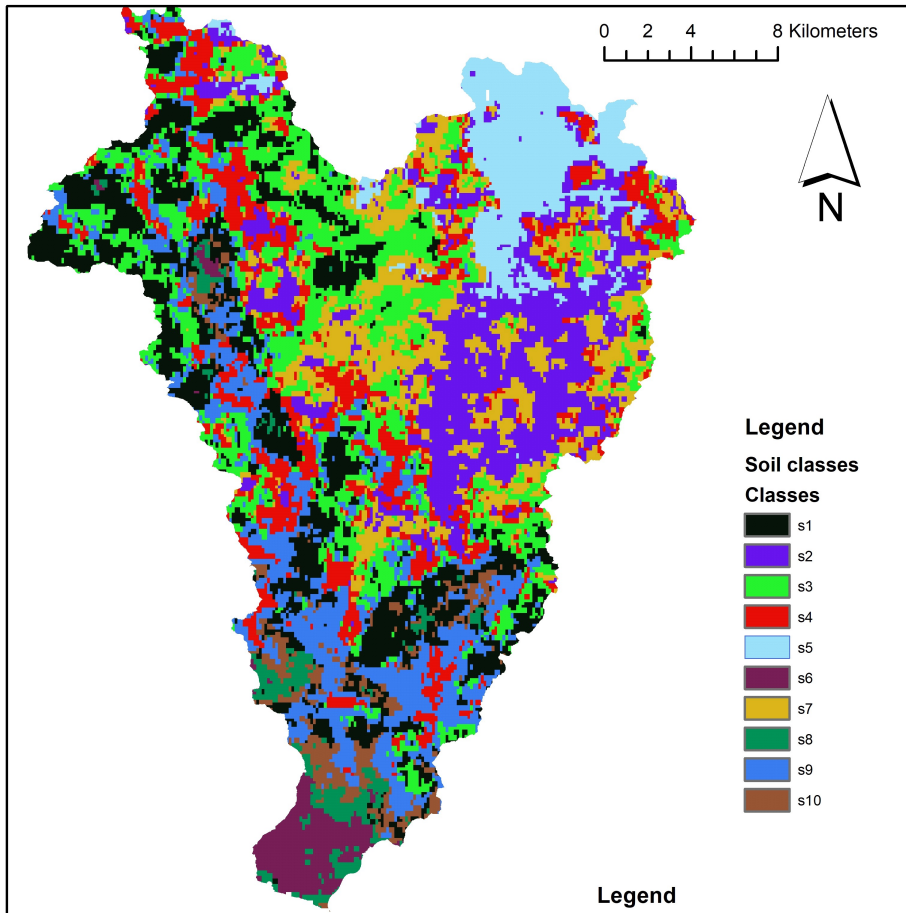


Figure 7 – Soil classes resulting from K-means clusterization algorithm

HRUs were delineated by setting thresholds of 50 ha on land use, soil and slope, in order to depict only dominant land uses and crop types within single sub-catchments. A total number of 297 HRUs has been identified corresponding to unique combinations of the elements listed in tables 3, 4 and 5. During the process of HRUs definition some of the crops with low area share in the catchment were lost.

In the process of HRUs definition also 4 elevation bands were created for each sub-catchment in order to simulate efficiently the snow processes in the catchment.

The main land use types (table 3) are evergreen forest and pasture. The generic land use pasture has been assigned the crop type “Tall fescue” (FESC) that is more suited for alpine-continental climates.

Table 3 – Land use distribution. Default SWAT crop parametrization was used.

Land use	Code	Area [ha]	% Wat. Area
Forest-Evergreen	FRSE	30326.51	49.04
Pasture	PAST	20672.57	33.43
Alsike Clover	CLVA	1229.917	1.99
Range-Brush	RNGB	57.4139	0.09
Residential-Low Density	URLD	1660.55	2.69
Winter Wheat	WWHT	1713.581	2.77
Range-Grasses	RNGE	366.4871	0.59
Forest-Mixed	FRST	4183.002	6.76
Corn Silage	CSIL	661.9704	1.07



Barren	BARR	73.3327	0.12
Corn	CORN	428.1274	0.69
Soybean	SOYB	200.25	0.32
Sugarbeet	SGBT	144.3309	0.23
Winter Barley	WBAR	116.0394	0.19

Table 4 – Soils distribution. Note: CLAY, SILT, SAND and CBN are values representative of the topsoil. CBN: fraction of organic carbon.

Soil	Area [ha]	%Wat.Area	CLAY [%]	SILT [%]	SAND [%]	CBN [%]
s1	10187.56	16.48	19	42	39	3.5
s2	10940.09	17.69	18	40	42	4.0
s3	9148.629	14.8	24	48	29	2.4
s4	8289.98	13.41	17	39	45	4.7
s5	5364.745	8.68	11	37	52	7.8
s6	1779.173	2.88	17	38	45	3.4
s7	7745.478	12.53	14	37	50	5.7
s8	642.8756	1.04	20	39	41	3.1
s9	6025.936	9.75	15	37	48	4.4
s10	1709.614	2.76	22	43	35	2.6

Table 5 – Slope distribution

Slope [%]	Area [ha]	%Wat.Area
0-15	29038.21	46.96
15-30	17104.79	27.66
30-9999	15691.07	25.38

2.5 Model structure

The SWAT model allows using different subroutines to simulate similar processes. The choice of such subroutines depends on the availability of data and on the specific case study.

Evapotranspiration is simulated using the Hargreaves method (Neitsch et al., 2011), that requires as input data only daily precipitation and maximum/minimum air temperature, whereas other methods (Pennmann-Montheith, Priestley-Taylor) require more input data (relative humidity, wind speed, solar radiation) without offering significant improvement in the estimation.

Runoff-infiltration split up is simulated with the daily curve number method and the Curve Number is adjusted daily based on soil moisture content (Neitsch et al., 2011).

Channel water routing is simulated using Muskingum method (Neitsch et al., 2011), with no evapotranspiration from the channel.

Sediment generation off-stream is modeled with the Modified universal soil loss equation (MUSLE), routing in the stream was modeled with the simplified Bagnold equation (Neitsch et al., 2011).

2.6 Weather data

Weather data for 15 weather stations were used in the model (Fig. 8), covering the period 1999 – 2017. Climate stations were discarded in case of lack of time coverage or in case of inconsistent data (e.g. too many gap in the daily time series).

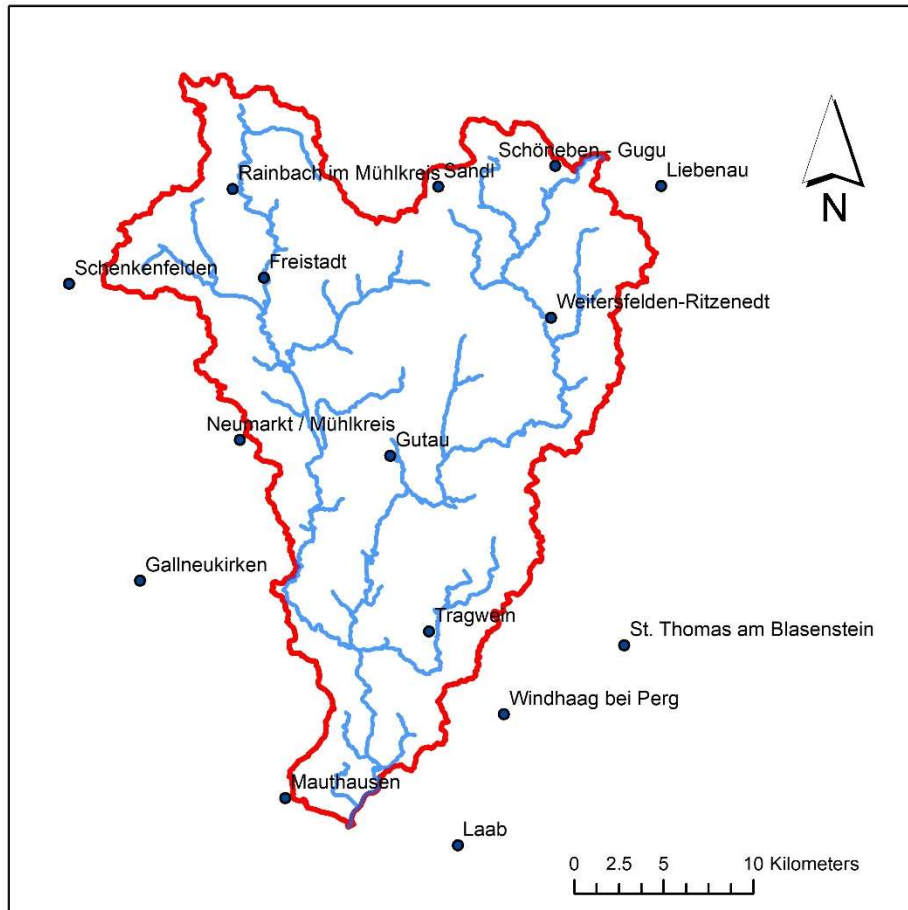


Figure 8 – Climate stations spatial distribution in the catchment.

The most sensitive parameter that drives the hydrological response of the model is precipitation. Therefore, special attention has been devoted to precipitation data preprocessing. Precipitation raw data has been processed multiple times:

- First, the inverse distance weighting algorithm (Bartier and Keller, 1996) was used to fill gaps in the records by using data from neighboring stations;
- Second, a gauge undercatch correction factor (Richter method, Sieck et al., 2007; Wagner, 2009) was used to adjust data to take into account the rain gauge undercatch issue.
- Third, inverse distance weighting was used for a second time to interpolate precipitation data into virtual rain gauges corresponding to the centroids of the subbasins. This is needed because the SWAT interpolation based on the nearest neighbour method is too simple and can lead to under/overestimation of precipitation for some subcatchments.

2.7 Point inlet

A point inlet was defined for the sub-catchment 6 in order to simulate the hydrological response of the part of the catchment that is not actually modeled (Fig. 9). The inlet daily flow data was

obtained by assuming a uniform distribution of the precipitation and a uniform response of the catchment to precipitation in the area upstream of the flow gauge station of Weitersfelden. The recorded mean daily flow observed in Weitersfelden gauging station was multiplied by the share of non-modeled area to the total area upstream the gauging station (approx. 30 %). The uncertainty involved in this procedure needs to be considered when the model performance is evaluated for the specific gauging station.

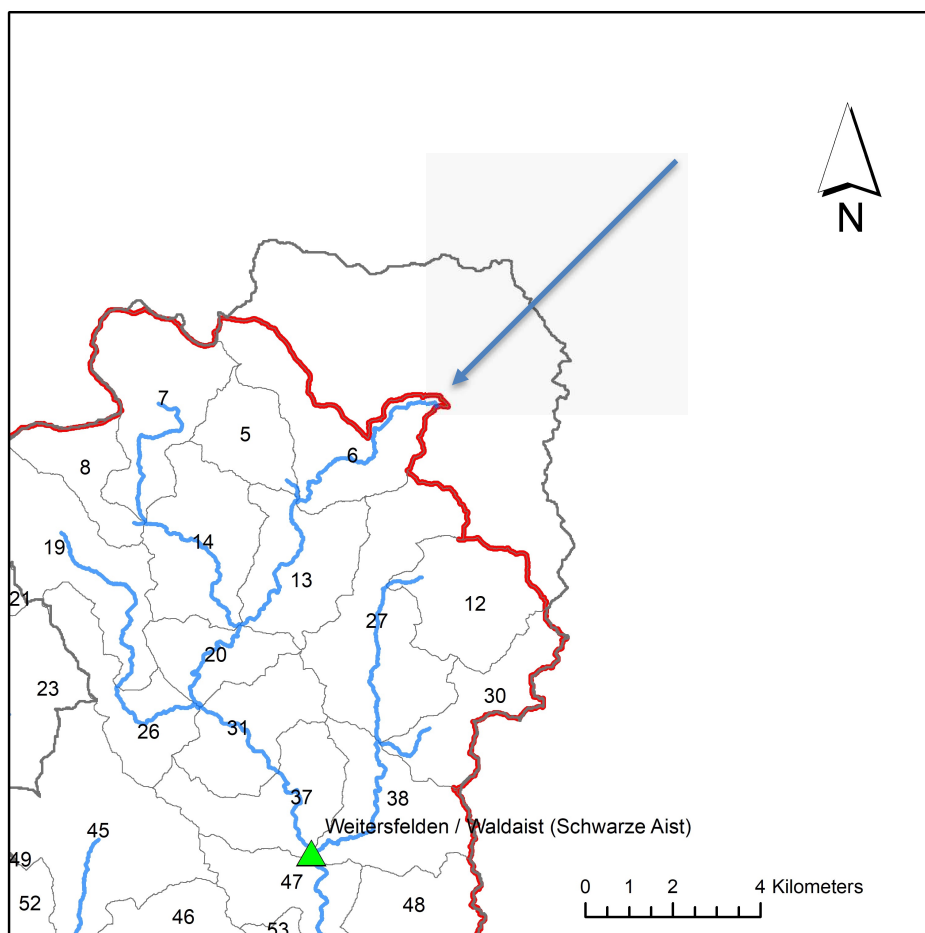


Figure 9 – Point inlet position

2.8 Ponds and reservoirs

Existing small water bodies were modeled in SWAT as equivalent ponds (one pond per sub basin). The volume of the ponds was estimated as a fraction of the ponds surface area. The fraction of the sub basin area that is draining into existing small water bodies was obtained using the TAUDem toolbox in ArcGIS (<http://hydrology.usu.edu/taudem/taudem5/index.html>) using as input data the ponds layer and the DEM.

2.9 Model calibration and validation for flow at the daily time step

The model was calibrated and validated using SWAT- CUP interface with daily flow data for 5 gauging stations (table 6, Fig. 10). The sequential uncertainty fitting (SUF12) algorithm was used for the optimization process. The calibration period was 2002 – 2010 (8 years) and the validation period was 2011 – 2015 (5 years). A warmup period of 3 years was used both for calibration and validation.

Table 6 – Flow gauging station names and position on SWAT subcatchments network

Gauging name	Reach	Corresponding sub-catchment
Freistadt	Feldaist	22
Kefermarkt	Feldaist	51
Weitersfelden	Waldaist	37
Pfahnmuele	Waldaist	84
Schwertberg	Aist	93

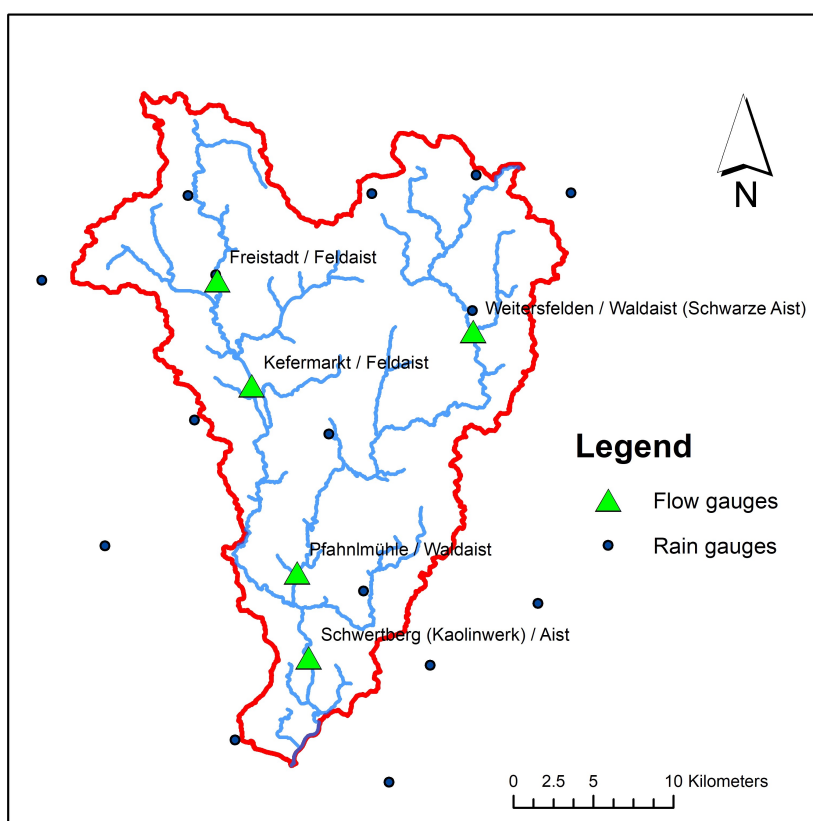


Figure 10 – Flow gauges location

The calibration procedure was carried out stepwise. The catchment was split into five regions corresponding to the sub-catchments between a gauging station and an upstream one. Flow – related parameters were calibrated independently for each of the regions upstream a gauging station. First the most upstream area was calibrated and, when a satisfactory match was obtained between observed data and modeled outputs, the parameters were frozen and the next downstream area was chosen for calibration.

The calibrated parameters and the starting ranges are related with groundwater processes, soil properties, snow processes, impoundments and runoff infiltration split-up, for a total of 27 parameters (Fig. 11). [Refer to Neitsch et al., 2012 for the physical meaning of the parameters]



r_CN2.mgt	-0.2	0.1		
v_GW_DELAY.gw	30	200		
v_ALPHA_BF_D.gw	0	0.2		
v_ALPHA_BF.gw	0	0.2		
v_GWQMN.gw	0	500		
v_GW_REVAP.gw	0.02	0.2		
v_REVAPMN.gw	400	1000		
v_RCHRG_DP.gw	0	0.05		
r_SOL_K().sol	-0.2	0.2		
r_SOL_AWC().sol	-0.2	0.2		
r_SOL_BD().sol	-0.2	0.2		
r_SLSUBBSN.hru	-0.15	0.15		
v_ESCO.hru	0.7	1		
v_EPCO.hru	0.01	1		
r_OV_N.hru	-0.2	0.2		
v_CH_N2.rte	0.01	0.3		
v_SUB_SFTMP().sno	-5	5		
v_SUB_SMTMP().sno	-5	5		
v_SUB_SMFMX().sno	1	8		
v_SUB_SMFMN().sno	1	8		
v_SUB_TIMP().sno	0.01	1		
v_PLAPS.sub	-1000	1000		
v_NDTARG.pnd	1	30		
v_PND_K.pnd	0	3		
r_PND_FR.pnd	-0.3	0.3		
r_SOL_ZMX.sol		FRSE, FRST	500	1500
r SOL_ZMX.sol		PAST, CLVA	300	1000

Figure 11 – List of parameters used for hydrology calibration. Note: v means the parameter change is absolute; r means the parameter change is relative to the value previously stored in the SWAT database.

The objective function that was maximized in the optimization procedure was the Klinge-Gupta efficiency (KGE, Gupta et al., 2009). Also Nash-Suthcliffe efficiency (NS) and Percent Bias (PBIAS) have been analyzed to check the consistency of the results.

The model calibration generally performed well (table 7), with higher fitting capacity for downstream stations and lower for most upstream gauges (Fig. 12, 14). This is due to the fact that the SWAT model runs with daily time steps and is generally not performing well in predicting runoff from small areas like those that are most upstream. Therefore the fitting capacity for Weitersfelden gauging station is not optimal both for calibration and validation.

However, the fitting capacity for the most downstream stations (Fig. 13, 14) is very good (Moriassi et al., 2007). The efficiency of fitting is a bit lower during the validation period, but still acceptable.

The complete list of the calibrated parameter values is reported in Appendix B.

Table 7 – Summary statistics for flow calibration and validation (KGE - Klinge-Gupta efficiency, NS - Nash-Suthcliffe efficiency, PBIAS - Percent Bias)

Gauge	SWAT sub	Calibration 2002 - 2010			Validation 2011 – 2016		
		NS	PBIAS	KGE	NS	PBIAS	KGE
Freistadt	22	0.64	-3.5	0.79	0.4	10.6	0.64
Weitersfelden	37	0.74	20.6	0.72	0.49	19.4	0.68
Kefermarkt	51	0.77	-8.4	0.82	0.57	12.7	0.75
Pfahlmühle	84	0.78	-1.1	0.88	0.62	2.2	0.81
Schwertberg	94	0.84	0.4	0.9	0.79	13.8	0.81

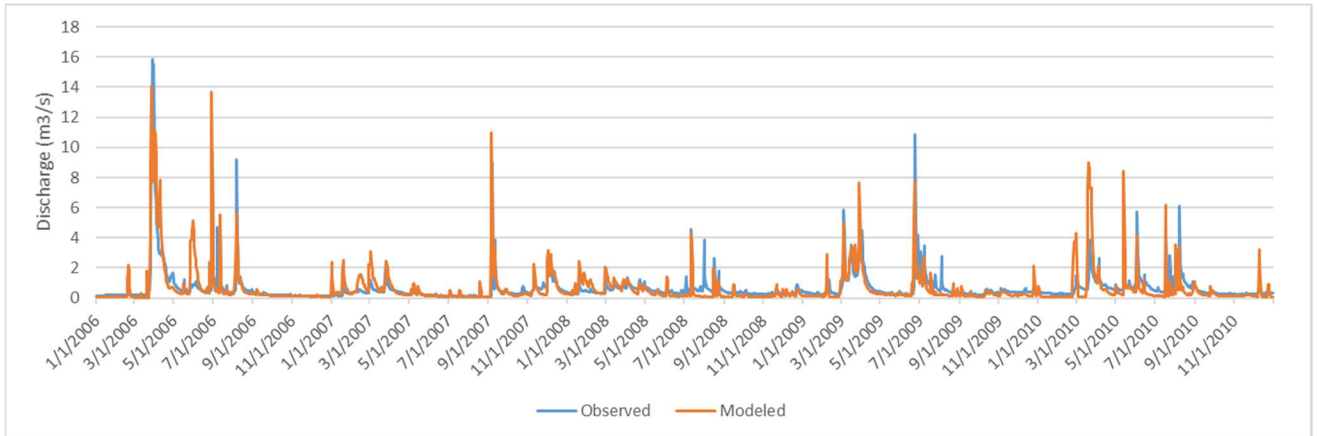


Figure 12 – Modeled vs. observed comparison for Freistadt gauging station; period 2006 – 2010.

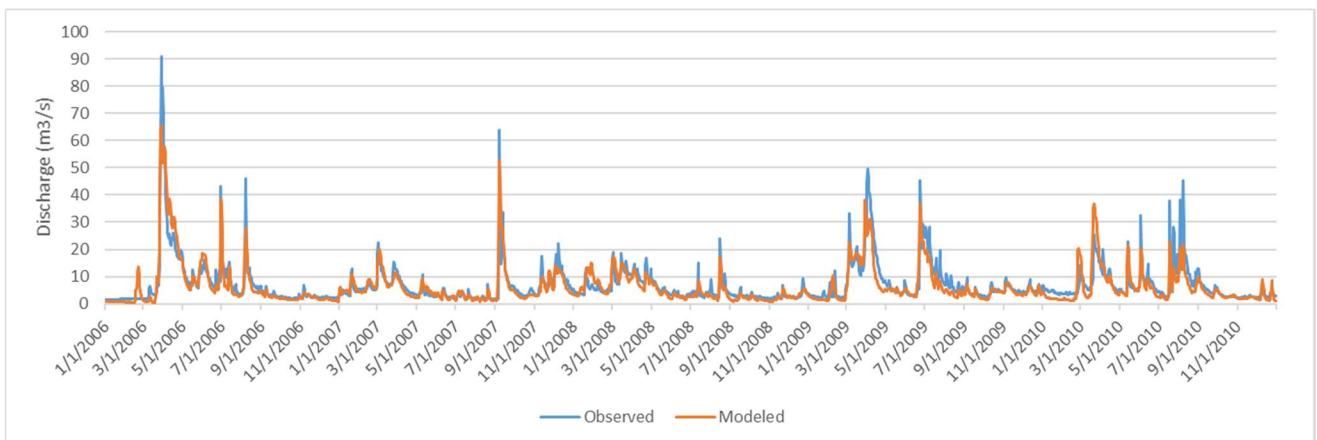


Figure 13 – Modeled vs. observed comparison for Schwertberg gauging station; period 2006 – 2010.

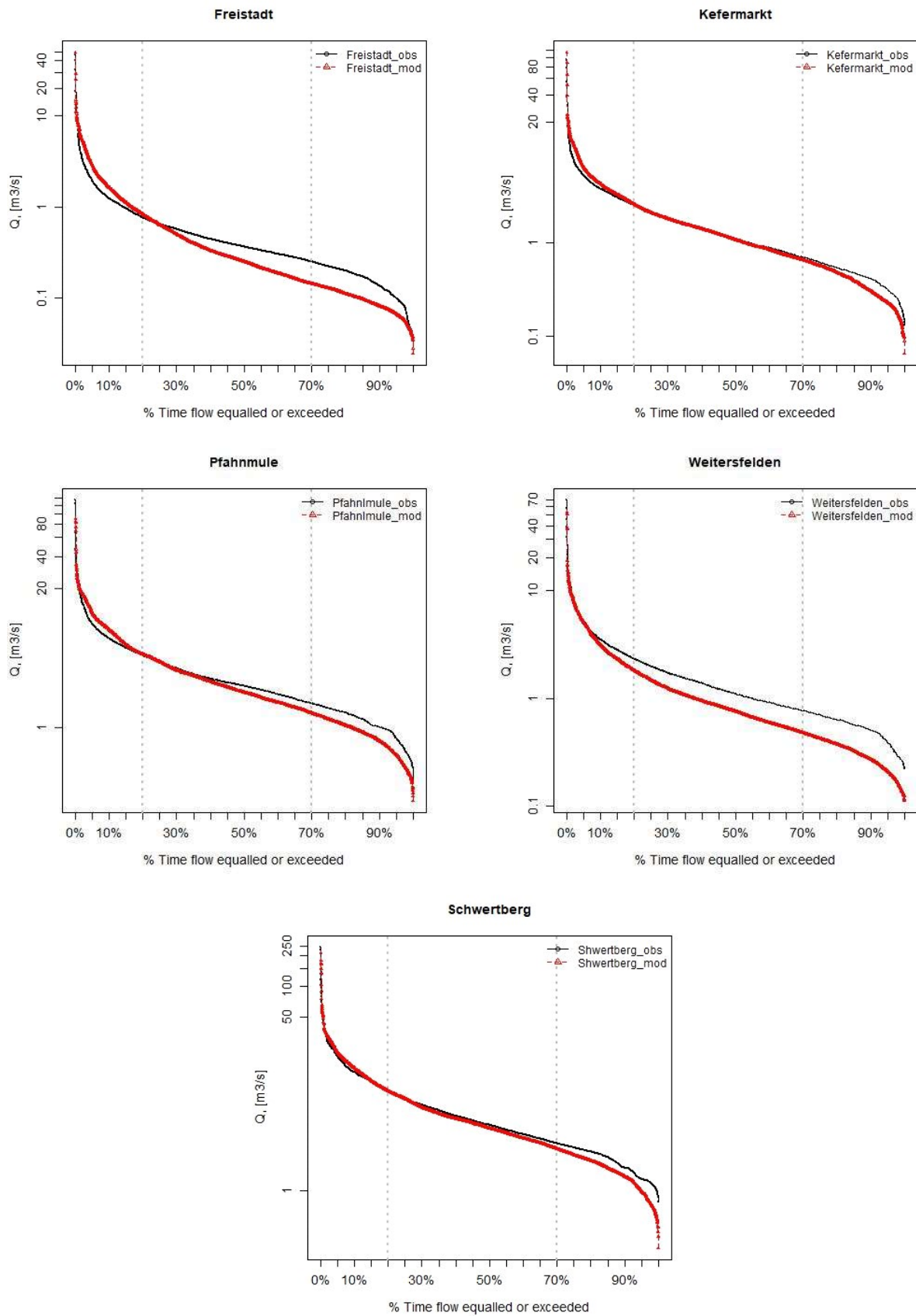


Figure 14 – Flow duration curves for the five gauging stations used for calibration.

2.10 Model calibration and validation for flow and sediment at the monthly time step

The SWAT model was calibrated and validated for sediment using SWAT- CUP interface with daily flow data for 7 sediment sampling stations (table 8, Fig. 15). The sequential uncertainty fitting (SUF12) algorithm was used for the optimization process. The calibration period was 2006 – 2010 (5 years) and the validation period was 2011 – 2015 (5 years). A warmup period of 3 years was used both for calibration and validation.

Available data from the water framework directive WFD monitoring program have been used for the calibration. Such data consist in bi-monthly collected samples (approx. 100 samples/year), details on the sampling procedure and on the analytic techniques can be found in: BLMFUW, 2017

Table 8 – Sediment sampling points position and corresponding subcatchment.

Gauging name	Reach	Corresponding subcatchment
Unterpasberg	Feldaist	2
Hihntermule	Feldaist	4
Freistadt	Feldaist	22
Flanitz	Feldaist	59
Pfahnmuele	Waldaist	84
Hohensteg	Feldaist	88

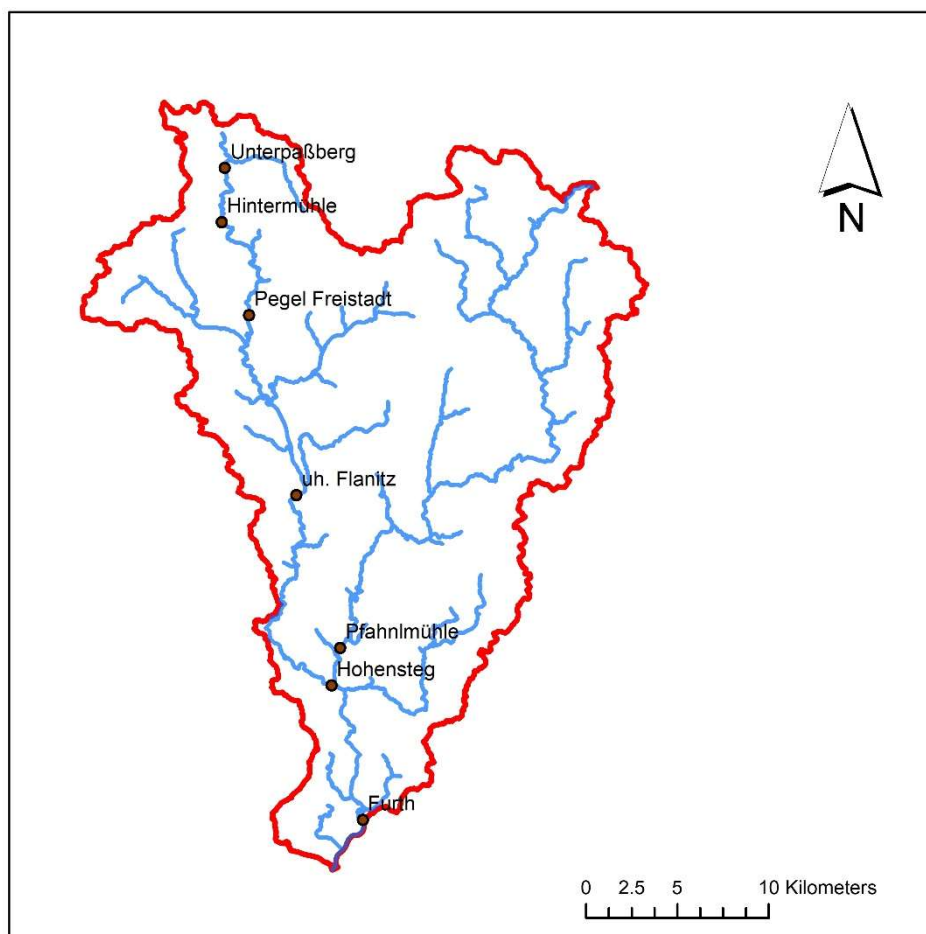


Figure 15 – Sediment sampling points



SWAT simulates sediment fluxes in a two-step process. First, sediments generation on the land are simulated at the HRU level using the Modified Universal Soil Loss Equation (MUSLE, Neitsch et al., 2012). Sediment generation on the land is a function of several factors: overland flow intensity, land use (USLE_C), soil structure (USLE_K), practices (USLE_P) and topographic factors. Sediment fluxes from the land phase are then routed into the stream network. SWAT simulates erosion/ deposition processes in the stream network with Bagnold simplified equation. Bagnold’s approach is based on the definition of a threshold separating deposition/resuspension conditions and on the concept of stream power.

Since available data do not take into account the subdivision between land and stream processes, but rather represent the sum of both contribution, a careful calibration should consider both effects.

It's important to stress out that some hydrological parameters are also affecting the sediment transport. For instance, the flow velocity in the channel drives the erosion/deposition patterns in the channels according to Bagnold’s equation: channel roughness and the channel width, associated with the hydrological component are affecting also the sediment budget of the channels. For this reason, a multi-site and multi-variable calibration was performed with a monthly time step, using as input database the hydrologically calibrated one and accounting in the objective function computation both the hydrological and the sediment variables. In total, 12 variables were accounted in the objective function definition, corresponding to the time series from 5 flow gauges and 6 sediment gauges.

The following steps were followed in the sediment calibration procedure:

- 1) Sediment samples data were preprocessed using LOADEST (Runkel et al., 2004; <https://water.usgs.gov/software/loadest/>) tool to compute monthly sediment loads.
- 2) Monthly averaged discharges were computed for each flow gauging station.
- 3) Sediment yields at the HRU level (land phase) were manually adjusted to be coherent with literature values found in Viagik et al. (2015). Crop operations (.mgt input file) were also adjusted.
- 4) SWAT-CUP was used with the adjusted database and both reach and land parameters were calibrated without any regionalization in order to use also basin scale parameters (.bsn input file) for calibration

The data preprocessing with LOADEST was successful. The predictors used to compute the flow characteristics were the discharge (using linear and quadratic terms) and the day of the year (using sinusoidal smoothing functions to account for loads yearly and seasonal periodicity). All the models proposed in the LOADEST documentation were tested and the best one was selected based on fitting capacity (minimize Akaike’s Information Criterion, AIC). The results were satisfactory for all the sediment sampling station (table 9). Generally downstream station have looser correlations, but Nash – Suthcliff efficiency (NSE) values are still acceptable (estimated loads are still better than using the mean multiannual loads).

Table 9 – LOADEST statistics for sediment sampling points. Bp = percent load bias; NSE = Nash – Suthcliff efficiency; PLR = (Bp + 100) / 100, partial load ratio.

Gauging name	Reach	Bb [%]	PLR	NSE	Mean load [t/d]
Unterpasberg	Feldaist	12.3	1.12	0.57	0.39
Hihntermule	Feldaist	3.82	1.04	0.78	0.92
Freistadt	Feldaist	-13.65	0.86	0.63	1.66
Flanitz	Feldaist	2.5	1.03	0.33	7.15
Pfahnmuele	Waldaist	-17.8	0.82	0.17	6.54
Hohensteg	Feldaist	-11.5	0.88	0.32	20.69

SWAT simulated daily discharge was used to prepare the loads to be used for sediments calibration because directly measured discharge for the sampling points was available only for the days when samples were collected. Sediment loads are increasing when moving downstream. The sediment loads from agricultural sub-catchments of the Feldaist river branch are higher than loads from the forested sub-catchments of Waldaist (table 9).

The uncalibrated SWAT model operations and crop types were adjusted to match observed sediment yields to realistic literature values. The uncalibrated adjusted values are in agreement with values reported in the literature for similar context. For instance, Viagik et al., 2015 reports values of sediment yield of 0.15 – 0.96 t/ha for forest, 0.12 – 1.96 t/ha for pasture and 0 – 4.3 t/ha for cropland in a Danube-scale application of the SWAT model.

The SWAT model was then calibrated for sediment using the SWAT-CUP program with a similar procedure to that used for the calibration of the hydrological component. The calibration focused on the transport of sediments in stream and left only USLE_C for some land uses (generic agriculture, corn, pasture and evergreen forest) as controlling parameter for upland erosion (Fig. 16). Refer to Neitsch et al., 2012 for the physical meaning of the parameters. A total number of 25 parameters was calibrated.

r__GW_DELAY.gw	-0.2	0.1
r__GWQMN.gw	-0.2	0.2
r__REVAPMN.gw	-0.2	0.2
r__RCHRG_DP.gw	-0.2	0.2
r__SOL_K().sol	-0.2	0.2
r__SOL_BD().sol	-0.3	0.3
r__SLSUBBSN.hru	-0.2	0.2
r__ESCO.hru	-0.2	0.2
r__OV_N.hru	-0.2	0.2
r__CH_N2.rte	-0.2	0.2
r__PLAPS.sub	-0.2	0.2
r__PND_K.pnd	-0.2	0.2
v__SURLAG.bsn	1	12
v__ADJ_PKR.bsn	1	10
v__SPEXP.bsn	1	2
v__PND_NSED.pnd	0	5000
v__PND_D50.pnd	5	10000
r__CH_W2.rte	-0.2	0.2
v__USLE_C{3}.plant.dat	0	0.1
v__USLE_C{5}.plant.dat	0	0.1
v__USLE_C{7}.plant.dat	0	0.1
v__USLE_C{8}.plant.dat	0	0.1
v__USLE_C{19}.plant.dat	0	0.1
v__PRF_BSN.bsn	1	2

Figure 16 – List of parameters used for hydrology and sediment combined calibration. Note: v means the parameter change is absolute; r means the parameter change is relative to the value previously stored in the SWAT database.

The multi-site and multi-variable calibration yielded satisfactory results for all the gauging stations (Table 10), with a mean KGE of 0.69 for calibration and 0.68 for validation, meaning that the model is not overfitting observed data and parameter ranges obtained in the calibration phase can be used also to extrapolate model results to other time periods.

The calibrated USLE_C values still provide upland erosion rates that are comparable with literature values (table 11). The erosion rate for evergreen forests is slightly higher than usual values, and is due to the intensity of forestry activities in the area, that leads to the mobilization to a huge amount of sediment (e.g. heavy machineries operations, clear-cutting, and construction of forestry roads). Calibrated parameters ranges are in appendix B.



Table 10 - Summary statistics for flow and sediment calibration and validation

Gauge	SWAT sub	Calibration 2005 - 2010			Validation 2011 - 2016		
		NS	PBIAS	KGE	NS	PBIAS	KGE
Freistadt	22	0.65	-7.1	0.73	0.64	-1.7	0.63
Weitersfelden	37	0.78	22.9	0.72	0.67	18.9	0.75
Kefermarkt	51	0.51	-5.5	0.56	0.74	7.8	0.85
Pfahnlmuele	84	0.69	-1.7	0.81	0.63	-5.7	0.77
Schwertberg	94	0.81	4.6	0.87	0.84	8.8	0.88
Unterpasberg	2	0.98	-0.2	0.98	0.95	-2.3	0.87
Hihntermule	4	0.69	37.2	0.39	0.68	27.7	0.47
Freistadt	22	0.81	-43.6	0.54	0.67	-45.9	0.53
Flanitz	59	0.82	5.7	0.67	0.73	-35.9	0.63
Pfahnlmuele	84	0.89	-17.3	0.72	0.92	-29.9	0.68
Hohensteg	88	0.66	23.4	0.43	0.52	15.3	0.43

Table 11 – sediment yield from implemented land uses uncalibrated values. CN = Curve number, the higher the curve number the higher the water infiltration. The table has been generated with the land use summary in the SWATcheck tool

Land use code	Land use	Area [km ²]	CN	Sediment Yield [t ha ⁻¹ y ⁻¹]
BERM	Bermuda switchgrass	16.6	67.91	0.06
CLVA	Red Clover	12.3	62.99	0.1
CORN	Corn	10.89	71.23	1.47
FRSE	Evergreen Forest	306.86	64.69	1.34
FRST	Mixed Forest	41.84	67.21	0.03
HAY	Hay	207.46	71.12	0.54
RNGB	Range Bushes	0.57	62.82	0.46
SGBT	Sugarbeet	1.44	71.5	0.79
SOYB	Soybean	2	73.76	2.5
WBAR	Winter barley	1.16	68.68	0.09
WWHT	Winter wheat	17.14	69.36	1.03

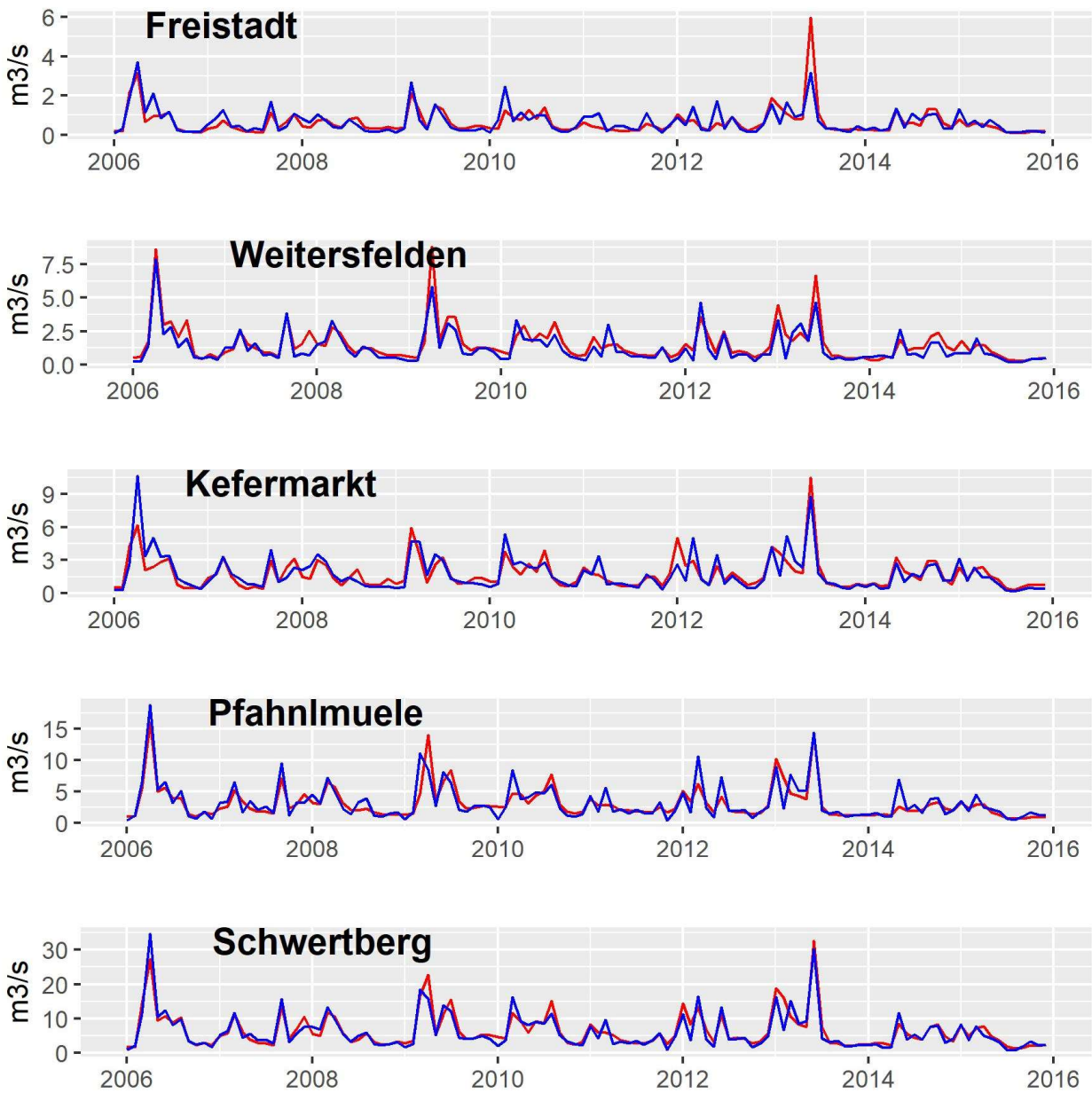


Figure 17 – Observed and modeled discharge for the flow stations the calibration and validation period

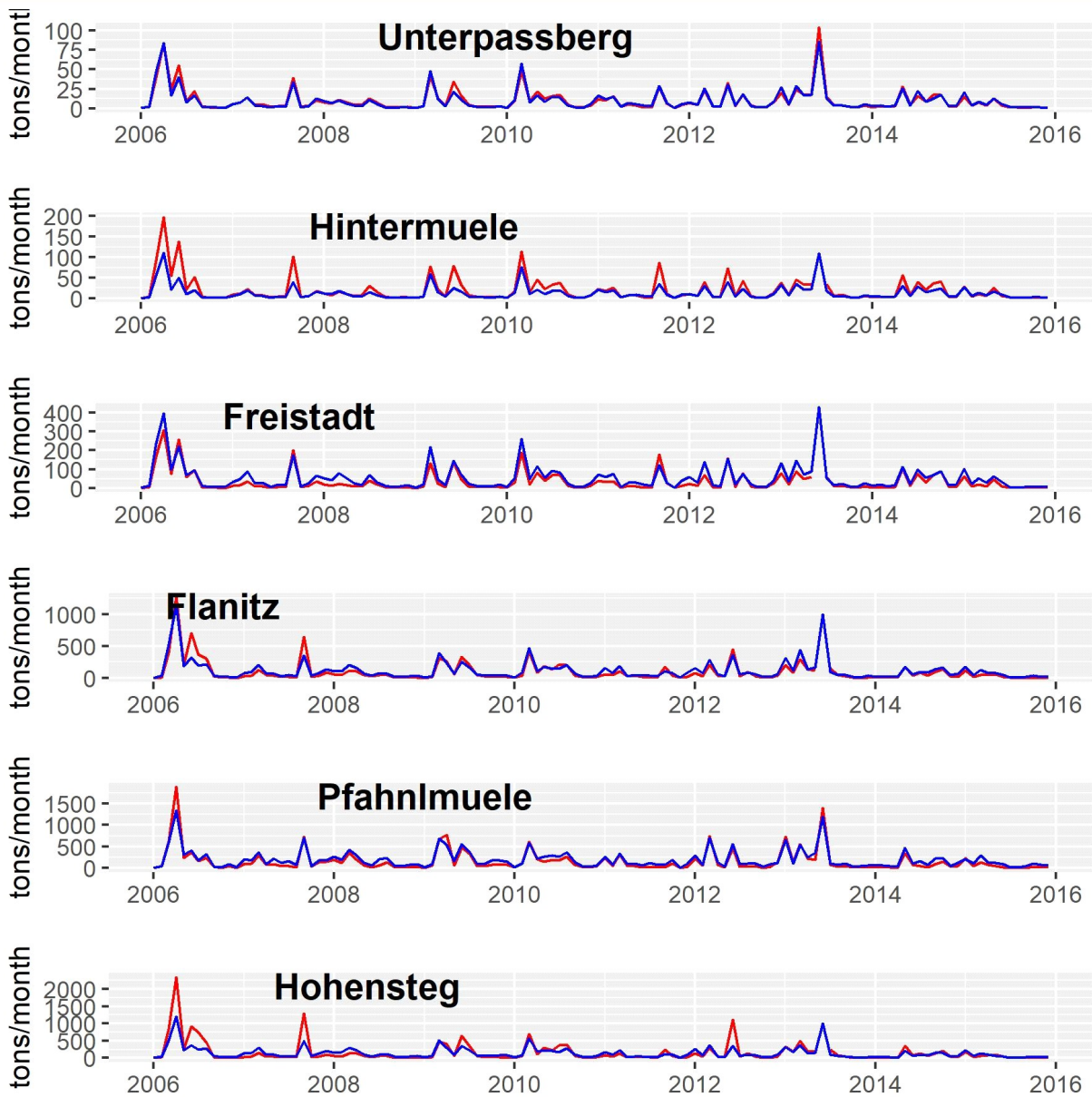


Figure 18- Observed and modeled sediment loads for the calibration and validation period



3. HYDRAULIC MODELING

The SWAT reach outputs are too coarse to provide information on the local hydraulic conditions. Therefore a hydraulic model has been used to downscale the coarse result to the meso-habitat scale.

A Hec-RAS hydraulic model developed by Hauer et al., 2015 was used for this purpose. The description of the detailed model setup is described in Hauer et al., 2015; in the following sections the main adaptations for the use of this model that have been done within the FRAMWAT project are summarized. The interface with SWAT is described since this has been developed within the FRAMWAT project.

The HEC-RAS modeling software calculates free-flow drainage in a watercourse using the one-dimensional St. Venant equations, based on a four-point implicit finite difference scheme. This allows the modeling of larger time steps compared to explicit numerical methods (Liggett & Cunge, 1975).

The Hec-RAS model was calibrated and validated with water level data collected on the field. Furthermore, the He-RAS model was used to assess siltation risk and was validated with siltation risk field data.

3.1 Description of the river network

For the preparation of the 1D discharge models, all rivers in the province of Upper Austria were taken into account that were also on the ministry map (Fig. 19). These rivers are overlapping with the river network delineated by SWAT (section 1.3) The two rivers Kolmbach and Muckenbach are located in the state of Lower Austria and due to a lack of data no 1D runoff model was created. In total, there are 19 streams (Table 12, Fig.19) with a total length of about 280 km for the 1D modeling.

Table 12 – River network modeled with HecRAS. Data from Hauer et al., 2015.

River	Channel	Length [km]
Feldaist	Prembach	4.5
	Gruenbach	3.7
	Schlager bach	3.4
	Kronbach	8.1
	Jaunitzbach	11.4
	Feistritzbach	15.5
	Lester Bach	6.5
	Flanitzbach	14.2
	Feldaist upstream	25.1
	Feldaist downstream	31.7
Waldaist	Flammbach	7.9
	Harbaist	10.2
	Fuchsreiterbach	4.5
	Weisse Aist	12.7
	Stampfenbach	10.5
	Klambach	6.1
	Waldaist upstream	28.0
Waldaist downstream	34.0	
Aist	Windegger Bach	7.3
	Kettenbach	21.8
	Aist	13.7
TOT		280.0

3.2 Geometric data

The 1D hydraulic models have been implemented with the 1D software program HEC-RAS 4.1 of the US Army Corps of Engineers (<http://www.hec.usace.army.mil/software/hec-ras/>). For model set-up in HEC RAS, it is necessary to enter the geometry of the rivers via cross sections and to assign roughness values to them.

The implemented hydrodynamic-numerical 1D-models are based on a digital elevation model (Airborne Laserscan, 1 m x 1 m, data source: Government of Upper Austria) and additionally sampled river stretches through bathymetric surveying of the Feldaist. The digital elevation model for the lower reach of the Feldaist and the Aist was provided by the Government of Upper Austria. However, hydraulic calculations on the Waldaist and tributaries (Table 1) could only be calculated on the basis of the digital elevation model (Airborne Laserscan, 1 m x 1 m, data source: Government of Upper Austria)

Based on the identified river network and orthophotos, the river axes are digitalized using HECGeo-RAS and cross-sections are created at a distance of approx. 25 m. In total, more than 11,000 cross-sections were created for 21 models (19 water bodies, the main channels of Feldaist and Waldaist were split into an upstream and a downstream reach). The Banks - embankment points in HEC RAS which border the channel on the left and right bank -were set manually for almost all cross-sections to specify the roughness area of a channel. At the same time, the banks are defined as those points where overflow from the river channel occurs when the bankfull water level is exceeded.

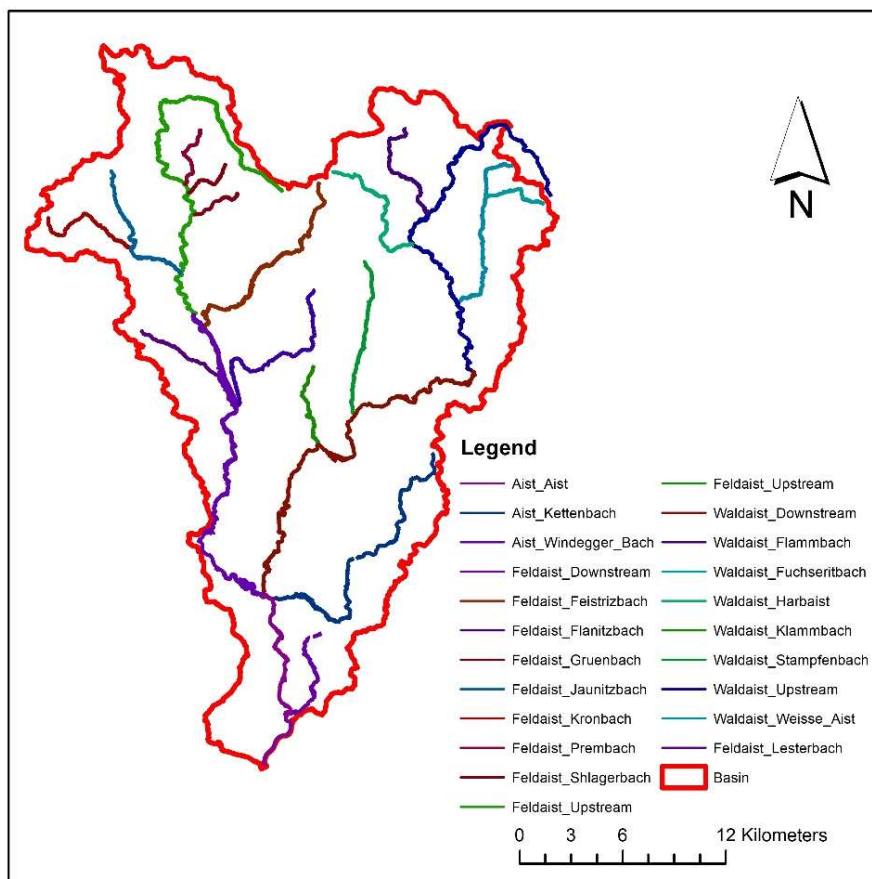


Figure 20 – HecRAS model spatial structure

Although only the discharge rates up to bankfull discharge are necessary for the evaluation of the results of the 1D runoff modeling, the Strickler and Manning roughness values were nevertheless determined for the foreland according to available data. Among other things, buildings were blocked out in accordance with the DKM in the 1D model. Thus, the created 1D discharge model can



also be used for high flows. The aim is to determine the discharge per cross-section with the help of 1D runoff modeling in HEC-RAS, where the calculated max. shear stress according to Mayer-Peter and Müller for sand is reached. As a result, possible transport and deposition areas for sand-like granite weathering material in a river stretch can be defined. These max. discharge values help to identify areas of risk for siltation.

3.3 Description of the model structure

The HecRAS model consists of 21 models (Table 13), one for each reach of the river network. The main channels of Waldaist and Feldaist were split into two reaches (Fig. 20). The reaches were modeled without junctions. Models have been calibrated for static flow profiles; therefore, all the simulations performed have used steady flow data.

Table 13 – Model structure description

Catchment	River	Length (km)	Number of cross sections	Mean profile distance
Feldaist	Prembach	4.5	178	25
Feldaist	Grünbach	3.7	146	25
Feldaist	Schlager Bach	3.4	134	25
Feldaist	Kronbach	8.1	321	25
Feldaist	Jaunitzbach	11.4	453	25
Feldaist	Feistritzbach	15.5	617	25
Feldaist	Lester Bach	6.5	258	25
Feldaist	Flanitzbach	14.2	561	25
Feldaist	Feldaist lower reach	25.1	979	26
Feldaist	Feldaist upper reach	31.7	1273	25
Waldaist	Flambach	7.9	314	25
Waldaist	Harbaist	10.2	396	26
Waldaist	Fuchsreiterbach	4.5	179	25
Waldaist	Weißer Aist	12.7	498	25
Waldaist	Stampfenbach	10.5	420	25
Waldaist	Klambach	6.1	239	25
Waldaist	Waldaist	61.0	2402	25
Aist	Windegger Bach	7.3	278	26
Aist	Kettenbach	21.8	853	26
Aist	Aist	13.8	533	26

3.4 Boundary conditions

As a boundary condition in HEC-RAS, the energy line gradient is chosen as input at the beginning and at the end of a model. For this, the mean bottom slope in the immediate area is calculated for both the model beginning and end and used as an approximation to the energy line gradient.

3.5 Hydrologic and hydraulic data

The discharge data used for the static profiles was obtained from SWAT simulations. The daily discharge for sub-catchment outputs was used to compute relative flow percentiles Q90, Q50 and Q20, which are high, medium and low flows indicators.

Q90 was selected as indicator for bankfull conditions after a manual check on single cross sections level to understand which flow percentile is representative of bankfull conditions. Q50 was selected as indicator for medium flows. Q50 can be also considered to be representative of channel forming discharge for gravel bed rivers, as the Aist system (see table 2 in Doyle et al., 2007).

The outputs of SWAT are available only for the outlet of each sub-catchment, while HecRAS requires information on the flow for every cross section. In order to simulate the gradual flow addition that occurs in the river network via lateral inflow, the output of each sub-basin was added as point inflow at specific cross sections of the river network (Fig. 21).

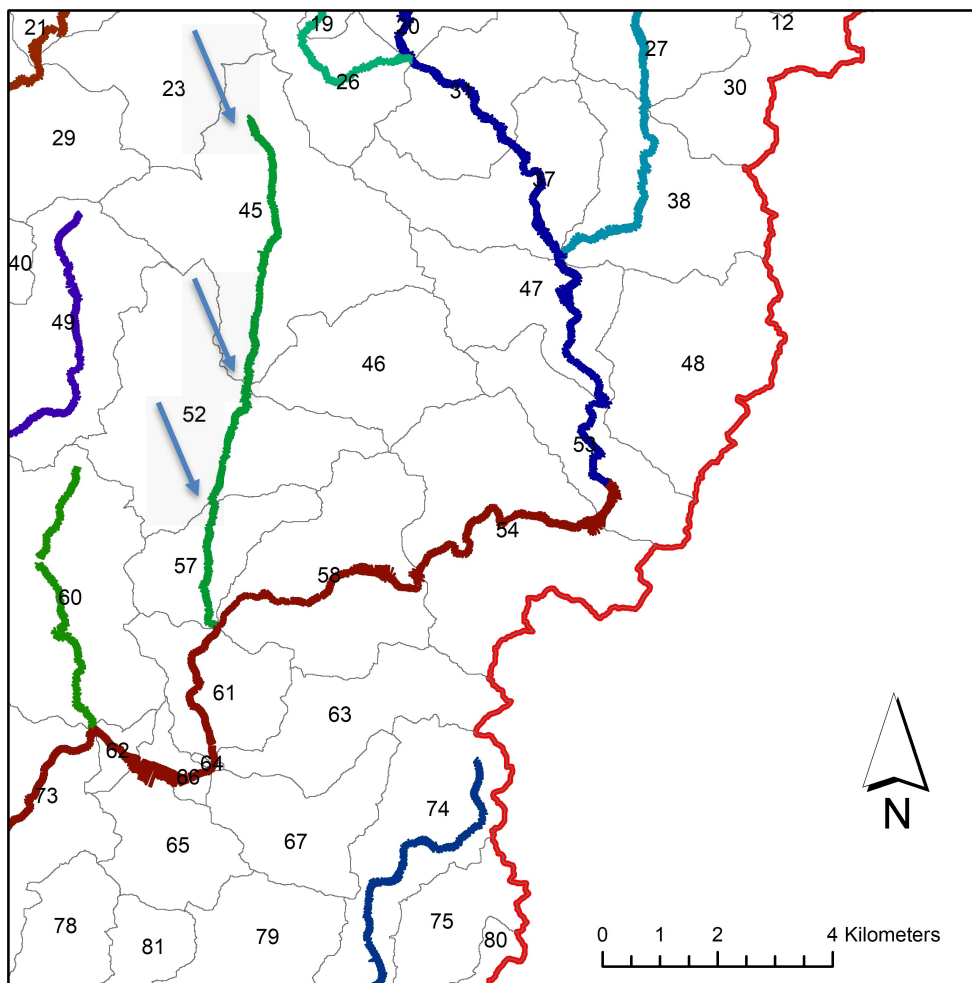


Figure 21 – SWAT subbasins and HecRAS river network overlay; point addition definition for HecRAS model for the Jaunitzbach reach that crosses subcatchments 45, 52 and 57 are represented by arrows.

The goodness of this approximation was tested in details for two HecRAS models: the Prembach, a small first order stream that is covered by a single SWAT sub-catchment (Fig 22) and the downstream stretch of the Waldaist river (Fig. 23), that has many tributaries and passes through many sub-catchments. Two different discharge addition method were tested:

- Step addition: a sudden increase of discharge was added to the specific cross section overlaying with SWAT sub-catchment outputs. This way the discharge in the stream in-



creases every time the HecRAS simulated reach crosses the output of a SWAT sub-catchment or every time there is a lateral inflow from a tributary.

- Continuous addition: the SWAT discharge is interpolated between two sub-catchment outlets for every cross section, simulating a continuous discharge inflow. This addition method allows for a continuous lateral inflow simulation and for step addition only in the cross sections where tributaries are contributing.

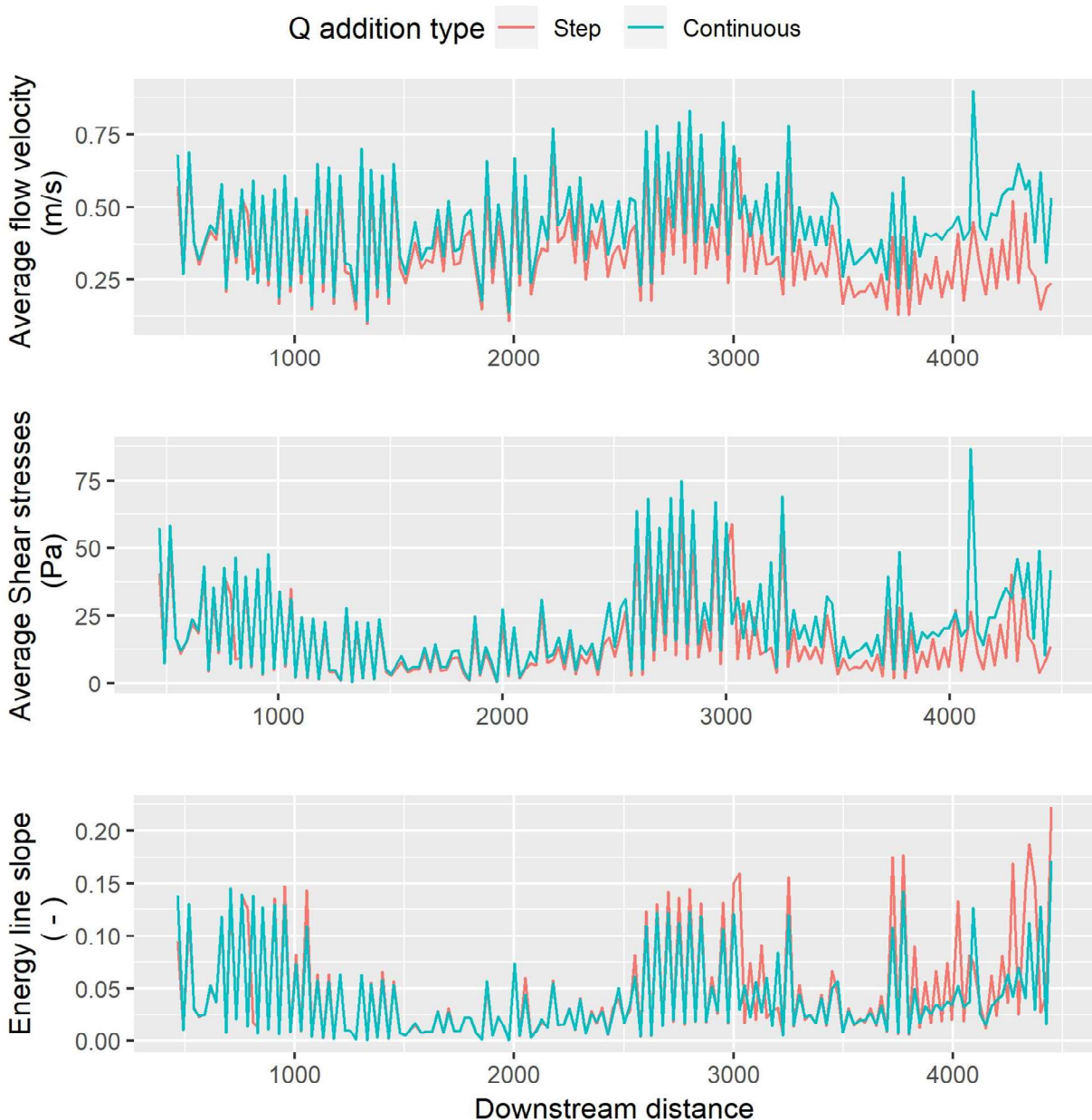


Figure 22 – Comparison between two different discharge addition methods (step and continuous) for the Prembach model. Note: the discharge at the upstream end of the channel was obtained by multiplying the discharge at the subcatchment outlet times the ratio of the point ending to the upstream area to the total subcatchment area.



The choice of the discharge addition method does affect the most upstream part of the Prembach model. Energy line slope and shear stresses are affected only in the upstream 500 meters. Flow velocity is more sensitive to the addition method and is affected significantly in the 1500 m upstream.

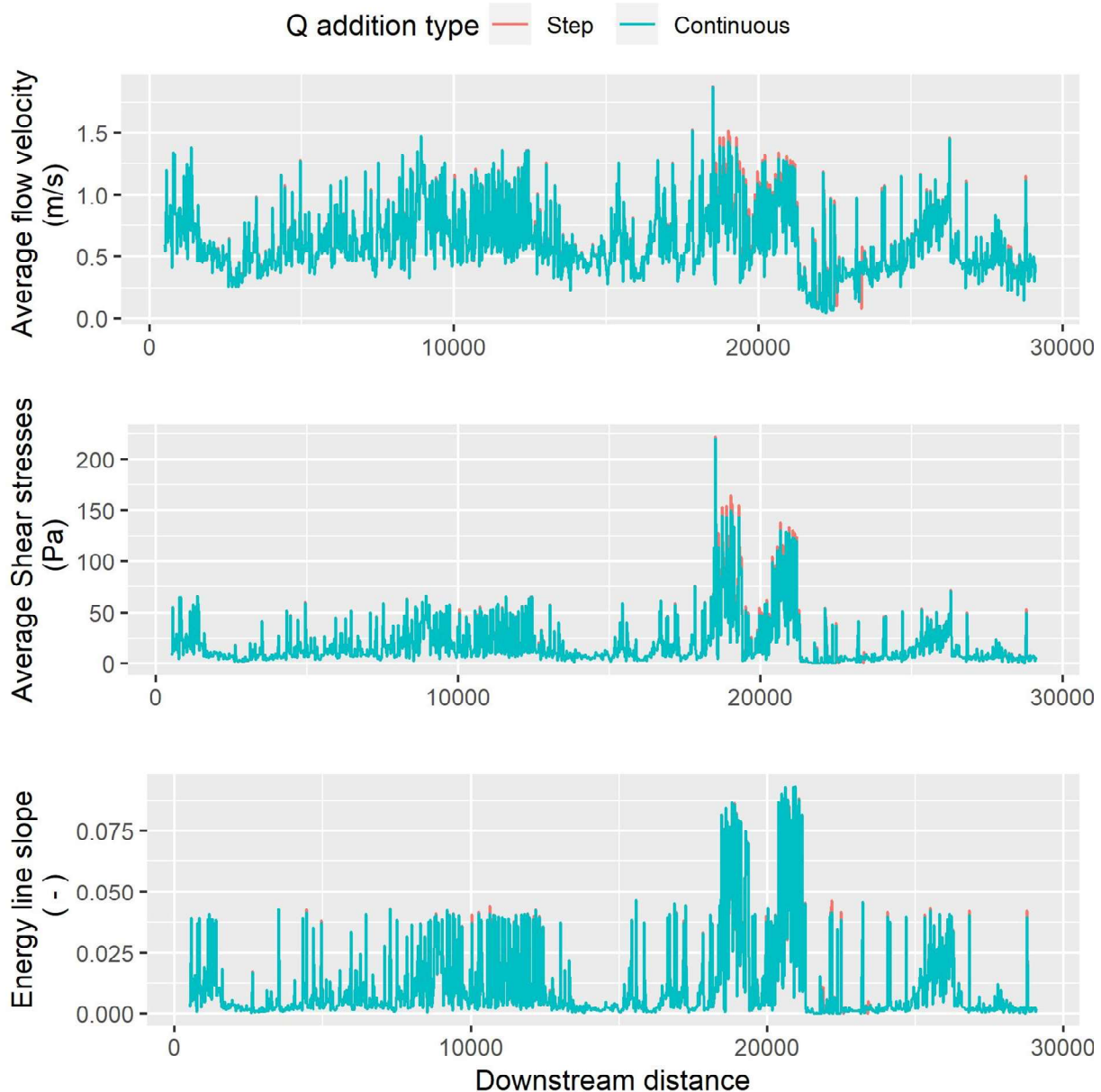


Figure 23 - Comparison between two different discharge addition methods (step and continuous) for the Waldaist Downstream model

3.6 Model calibration and validation

After creating the geometry data, the roughness is determined according to Strickler (kST) or Manning ($n = 1 / kST$) for the foreland and the river channel. For the model areas with the laser scan data, a slightly revised landscape survey map is used for the foreland. For this purpose, built-up area



were added to the soil function map and subsequently 6 roughness classes were created and roughness values were assigned according to literature.

The model was calibrated by adjusting the k_{ST} values in order to minimize the differences between measured and modeled water depth and flow velocity. An example of the procedure is described in Fig. 24. For further details, refer to Hauer et al., 2015.

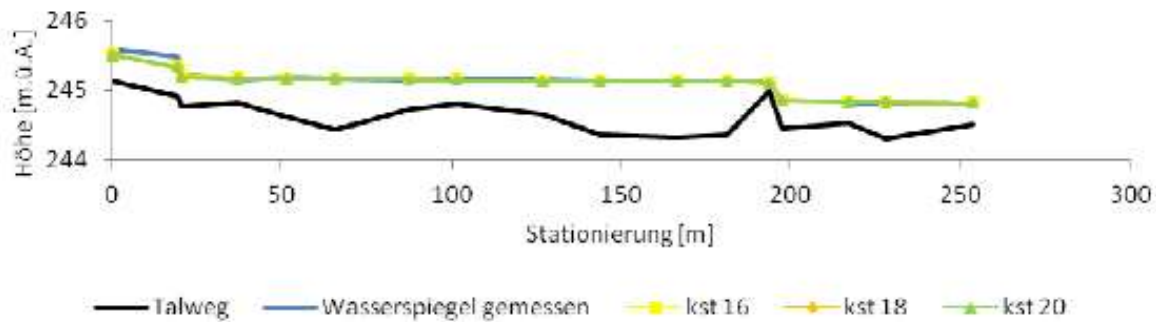


Figure 24 – Observed vs modeled water level used for k_{ST} calibration

The difference between the calculated and measured water surface elevation is a maximum of 3 cm. This calibration approach can be found in the literature among others in Bolla Pittaluga et al. (2014), Gomez et al. (2007) and Miori et al. (2006). In those sections where only airborne laserscan data were available a sensitivity analysis was performed.

3.7 Model uncertainties

Airborne Laser Scanning (ALS) technology was used to generate the DEM used for cross sections definition. However, without the use and evaluation of a green laser, the laser is reflected at the water surface and therefore the riverbed cannot be displayed. In addition, the ALS surveys were conducted at relatively high water levels and, due to the higher water level, higher inaccuracy may also occur. The main channel of the Feldaist was corrected with elevation data collected on the field, whereas the Waldaist was not corrected.



4. HYDROLOGICAL, HYDRAULIC AND SEDIMENT PREDICTORS

Indicators of hydrological alteration (IHAs) were used to generate ecologically relevant predictors from the daily hydrograph describing duration, frequency, timing, magnitude and rate of change of flow events (Olden and Poff, 2003). The R package ‘EflowStats’ was used to calculate the complete set of 171 IHAs corresponding to SWAT sub-catchments outlets. One metric for each category was selected to minimize the predictors’ redundancy with a pairwise collinearity analysis and a principal component analysis. When the pairwise correlation exceeded the 0.7 threshold, the metric with the lower loading on the most significant axis was removed from the list (Kakouei et al., 2017).

Magnitude IHAs were excluded from the analysis because implicitly they are already used in the calculated flow percentiles. Shortlisted IHAs were assigned to the reach upstream of the sub-catchment outlet they were computed for.

SWAT sediment outputs were averaged for each sub-catchment and normalized for channel length:

$$S_{i,p} = S_{SWAT,i,p} \frac{A_i}{L_i}$$

Where, for sub-catchment i and load percentile p : $S_{i,p}$ is the sediment load to the channel (t km⁻¹), $S_{SWAT,i,p}$ is the SWAT sediment (t ha), A_i is the area of the subcatchment (km²), L_i is the length of the channel (km). Two versions of S_i were computed, a local one and a cumulative upstream one.

HecRAS cross-sections outputs including several hydraulic parameters, including flow velocity (m s⁻¹), flow depth (m), Froude number (-) and shear stress (Pa) were used as predictors. Finally, the riparian land use for each HecRAS cross section was calculated as fractions of agricultural, pasture, forested and urban land uses in 100 m circular buffer.

All the predictors were resampled at a 50 m resolution and rasterized to produce the environmental layers for RF and SDMs (table 14). A time window with a length of 10 years was selected to calculate time-independent predictors averaged values.

Hydrological and sediment predictors were calculated at the sub-catchment level without any spatial interpolation, since the reduced sub-catchments dimension implies a homogeneous hydrograph response.



Table 14 – Predictors extracted from SWAT, HecRAS and the land use map

Short name	Name	Description	Units	Source
LTs_up	Upstream mean sediment load	SWAT sediment yield in the simulation period normalized by the drainage density, 50 th percentile	t km ⁻¹ month ⁻¹	SWAT
LTs_up_90	Upstream peak sediment load	SWAT sediment yield in the simulation period normalized by the drainage density, 90 th percentile	t km ⁻¹ month ⁻¹	SWAT
LTs_lc	Riparian mean sediment load	SWAT sediment yield in the simulation period normalized by the drainage density, 50 th percentile	t km ⁻¹ month ⁻¹	SWAT
LTs_lc_90	Riparian peak sediment load	SWAT sediment yield in the simulation period normalized by the drainage density, 90 th percentile	t km ⁻¹ month ⁻¹	SWAT
dh3	Annual maxima of 7-day means of daily discharge	Magnitude of maximum annual flow for weekly duration	m ³ d ⁻¹	SWAT
d115	Low exceedance flow	Mean magnitude of flows exceeded 90% of the time divided by median daily flow, over all years	-	SWAT
fl2	Variability in low flow pulse count	Coefficient of variation of number of annual occurrences during which the magnitude of flow remains below a lower threshold. Pulses are defined as those periods within a year in which the flow drops below the 25 th percentile of all daily values for the time period	-	SWAT
fh5	Flood frequency	Mean number of high flow events per year using an upper threshold of 1 time the median flow over all the years	-	SWAT
ta2	Predictability of flow	Sum of constancy and contingency of the flow (Colwell, 1974)	-	SWAT
ra2	Variability in rise rate	Coefficient of variation of the mean rate of positive changes in flow from one day to the next	-	SWAT
v_LF	Flow velocity during low flow	Cross sectional average of flow velocity; from an HecRAS static flow profile with a flow equal to the 20 th percentile of all daily flow	m s ⁻¹	HecRAS
v_MF	Flow velocity during mean flow	Cross sectional average of flow velocity; from an HecRAS static flow profile with a flow equal to the median value of all daily flow	m s ⁻¹	HecRAS
v_HF	Flow velocity during high flow	Cross sectional average of flow velocity; from an HecRAS static flow profile with a flow equal to the 90 th percentile of all daily flow	m s ⁻¹	HecRAS
v_rng	Flow velocity range	Absolute difference between v_HF and v_LF	m s ⁻¹	HecRAS
F_LF	Froude number during low flow	Cross sectional average of Froude number; from an HecRAS static flow profile with a flow equal to the 20 th percentile of all daily flow	-	HecRAS
F_MF	Froude number during mean flow	Cross sectional average of Froude number; from an HecRAS static flow profile with a flow equal to the median value of all daily flow	-	HecRAS
F_HF	Froude number during high flow	Cross sectional average of Froude number; from an HecRAS static flow profile with a flow equal to the 90 th percentile of all daily flow	-	HecRAS
F_rng	Froude number range	Absolute difference between F_HF and F_LF	-	HecRAS
SS_LF	Shear stresses for low flow	Cross sectional average of shear stresses; from an HecRAS static flow profile with a flow equal to the 20 th percentile of all daily flow	Pa	HecRAS
SS_MF	Shear stresses during mean flow	Cross sectional average of shear stresses; from an HecRAS static flow profile with a flow equal to the median value of all daily flow	Pa	HecRAS
SS_HF	Shear stresses during high flow	Cross sectional average of shear stresses; from an HecRAS static flow profile with a flow equal to the 90 th percentile of all daily flow	Pa	HecRAS
SS_rng	Shear stresses range	Absolute difference between SS_HF and SS_LF	Pa	HecRAS
d_LF	Flow depth for low flow	Cross sectional average of flow depth; from an HecRAS static flow profile with a flow equal to the 20 th percentile of all daily flow	m	HecRAS
d_MF	Flow depth during mean flow	Cross sectional average of flow depth; from an HecRAS static flow profile with a flow equal to the median value of all daily flow	m	HecRAS
d_HF	Flow depth during high flow	Cross sectional average of flow depth; from an	m	HecRAS



		HecRAS static flow profile with a flow equal to the 90 th percentile of all daily flow		
d_rng	Flow depth range	Absolute difference between d_HF and d_LF	m	HecRAS
SPs_LF	Specific stream power for low flow	Cross sectional average of specific stream power*; from an HecRAS static flow profile with a flow equal to the 20 th percentile of all daily flow	W m ⁻¹	HecRAS
SPs_MF	Specific stream power during mean flow	Cross sectional average of specific stream power*; from an HecRAS static flow profile with a flow equal to the median value of all daily flow	W m ⁻¹	HecRAS
SPs_HF	Specific stream power during high flow	Cross sectional average of specific stream power*; from an HecRAS static flow profile with a flow equal to the 90 th percentile of all daily flow	W m ⁻¹	HecRAS
SPs_rng	Specific stream power range	Absolute difference between SPs_HF and SPs_LF	W m ⁻¹	HecRAS
LU_FR_rip	Riparian forest	Fraction of forest land use in a circular buffer with 200 m radius from the river raster cell	-	Land use map
LU_AG_rip	Riparian agricultural area	Fraction of agricultural land use in a circular buffer with 200 m radius from the river raster cell	-	Land use map
LU_PA_rip	Riparian pasture area	Fraction of pasture land use in a circular buffer with 200 m radius from the river raster cell	-	Land use map
LU_UR_rip	Riparian artificial/sealed area	Fraction of artificially sealed/urban land use in a circular buffer with 200 m radius from the river raster cell	-	Land use map

* the specific stream power was calculated out of HecRAS outputs with the following formula:

$$SPs = \frac{\rho g Q S}{b}$$

Where: ρ is the density of water (1000 kg m⁻³), g is the gravity acceleration (9.81 m s⁻²), Q is the discharge (m³ s⁻¹), S is the channel slope and b is the channel width (m)

5. SILTATION MODEL

Random Forest models (Breiman, 2001) were used to fit the observed sand accumulation class with hydrological, hydraulic and sediment predictors. The survey and assessment of the degree of siltation was carried out by river channel mapping and volumetric sampling of the substrate. The mapping was carried out between December 2013 and July 2014 according to the hydro morphological status of a water body under the WFD (LAWA, 2000; BMLFUW, 2010). For this purpose, the local silting magnitude was classified into 4 classes according to the extent of mesohabitat alteration by siltation (siltation risk ranging from 0 to 3+ where 0 corresponds to undisturbed conditions and 3+ to moving sand substrate, figures 26 and 27). The input dataset was split in a calibration set (70%) and validation set (30%).

The calibration dataset was used with a 10-fold cross validation to tune the model's hyperparameters (Strobl et al., 2009) and fit the RF. Features were selected using the approach described by Haddachi et al. (2018): a short list of 8 predictors was selected among the available predictors based on expert opinion and used for fitting, while the 'VSURF' R package (Genuer et al., 2015) was used to detect redundant predictors. Only variables useful for interpretation were retained. Predictors importance in the final model was assessed as the mean decrease in accuracy when the predictor is randomly permuted (Breiman, 2001). The model goodness was evaluated using the accuracy (ACC), Kappa index, and true skill statistics (TSS) derived from the testing dataset confusion matrix.

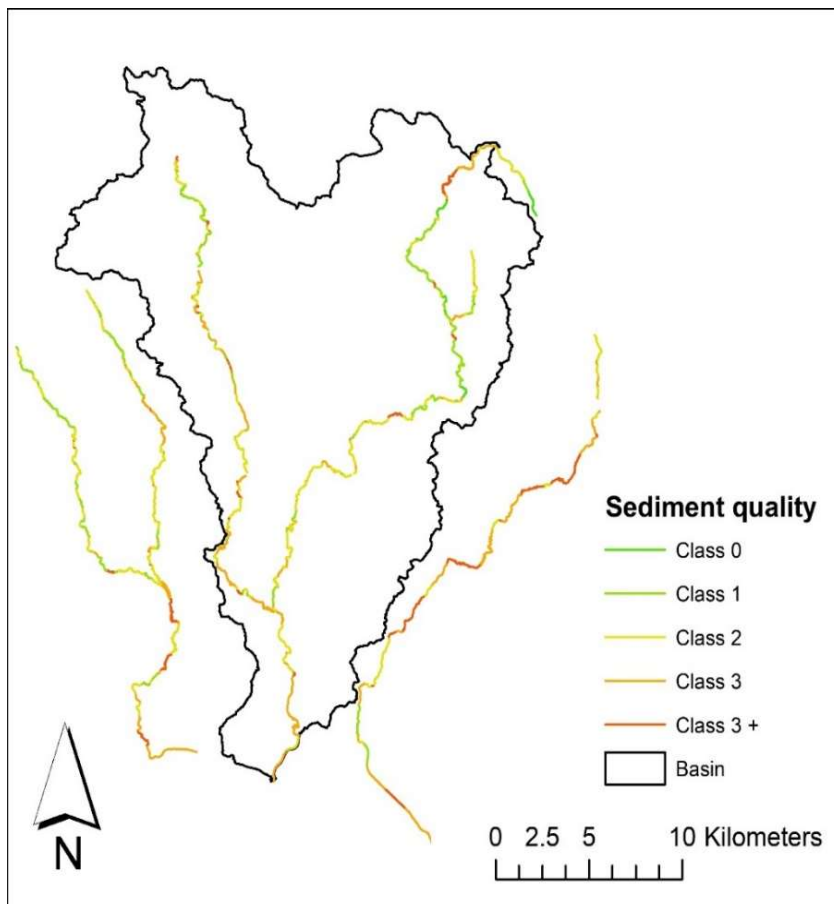


Figure 25 – Mapped siltation risk in the Aist catchment. Data collected between December 2013 and July 2014. Refer to Hauer et al., 2015 for the detailed sampling scheme.

Note: in this report the terms siltation, fines accumulation and sand accumulations are used as synonyms and refer to accumulations of sediments with a mean diameter between 1 and 10 mm that are resulting from the erosion of the granitic substrate. Refer to Hauer et al., 2015; Leitner et al., 2015; Scheder et al., 2015 for further details on the siltation issue in the region.

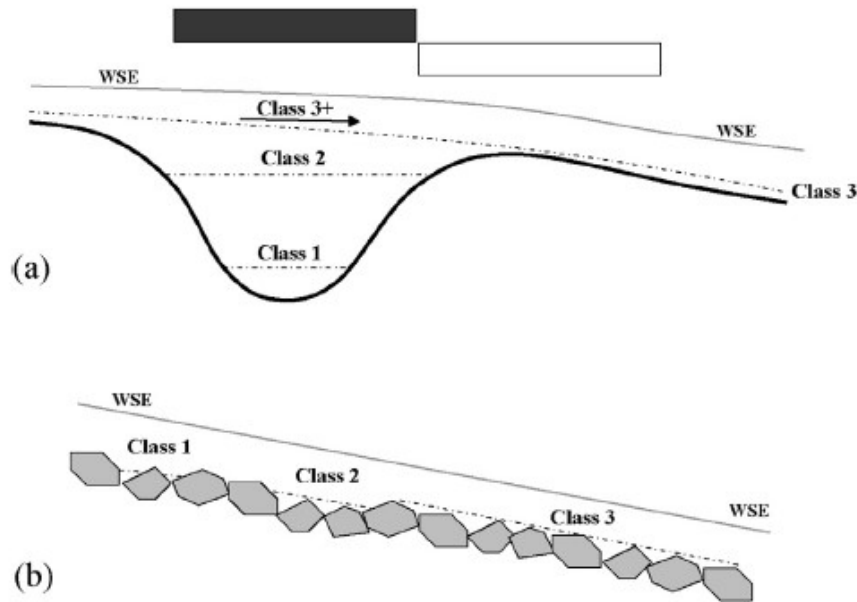


Figure 26 – changes in river morphology due to sediments accumulation for a) riffle (white bar) and pool (black bar) and b) plane bed. 1: no disturbance; 2: habitat changes are obvious but important morphological characteristics are still given, 3: significant habitat degradation; 4: significant habitat degradation and sediment mobilization under medium flow conditions. WSE: water surface elevation. The picture is from Hauer et al., 2015.

The siltation model based on RF showed a good discriminatory capacity (test performance metrics: ACC = 0.72, Kappa = 0.60). Variables affecting most the reach siltation status are the cumulated upstream sediment loads, the frequency of high flows and the high flow shear stresses. Most of the catchment area (37%) falls into moderate risk (class 2); whereas high siltation risk classes 3 and 3+ occupy respectively 14% and 4% of the reach cells.



6. HABITAT MODEL

A habitat model based on univariate habitat suitability indices was set up. Univariate habitat suitability indices are a simple modeling technique that relies on collected field data to describe the physical habitat requirements of a target organism.

The target organism used for the habitat model is the Freshwater Pearl Mussel (FPM, *Margaritifera margaritifera*). FPM is an endangered organism and only few populations are left in the Aist catchment because of fine sediments accumulation and climate-change induced alterations in flow regime. (Hauer et al., 2015).

6.1 Field data

Field data collected in several field surveys were used. The bigger datasets used were obtained from: *Huemer, D., C. Scheder, D. Csar & C. Gumpinger (2016): Kurzbericht zur Muschelkartierung in der Waldaist. Bericht im Auftrag der Abteilung Naturschutz am Amt der Oberoesterreichischen Landesregierung, Wels, 6 S. und Karten.*

Available field data points were snapped to the closest HecRAS cross section. When multiple sampling points were close to the same cross section, the sum of the individuals was computed. Most of the data points available count less than 5 individuals, but some of them account for populations up to several hundreds of individuals (fig. 28).

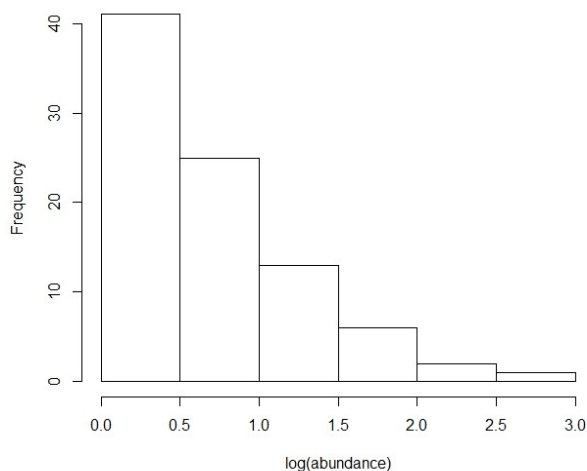


Figure 27 – Distribution histogram of the available Freshwater pearl mussel data

6.2 Habitat suitability indices derivation

The habitat suitability curves have been obtained using hydraulic predictors from HecRAS simulations. Flow velocity, average flow depth, shear stresses and Froude number for low flow (Q20), mean flow (Q50) and high flow (Q90) were extracted for every cross section where abundance/density data were available. Collinearity was tested and a subset of 3 predictors was selected to continue the analysis: flow velocity for low flow, flow velocity for high flow and shear stresses for mean flow.

The method is described in detail in Hastie et al., 2000. Habitat availability was determined by grouping the investigated cross sections into classes (fig. 29, 30, and 31). Habitat utilization was determined by counting the number of individuals belonging to each habitat class. Habitat preference was the normalized ratio between habitat preference and habitat availability.

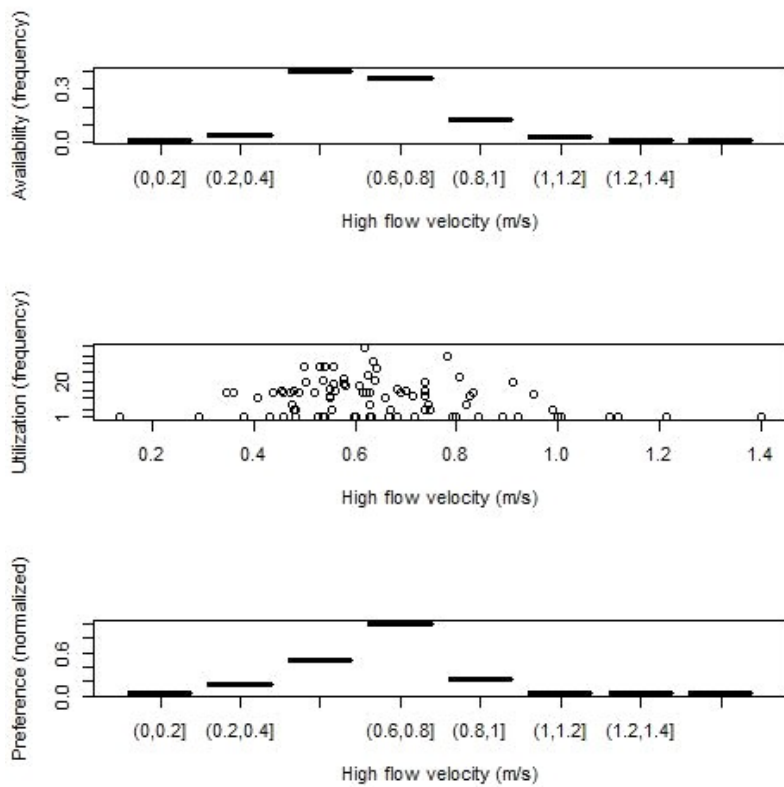


Figure 28 – Habitat availability (up), individuals utilization (middle) and habitat preference (bottom) for Q90 flow velocity.

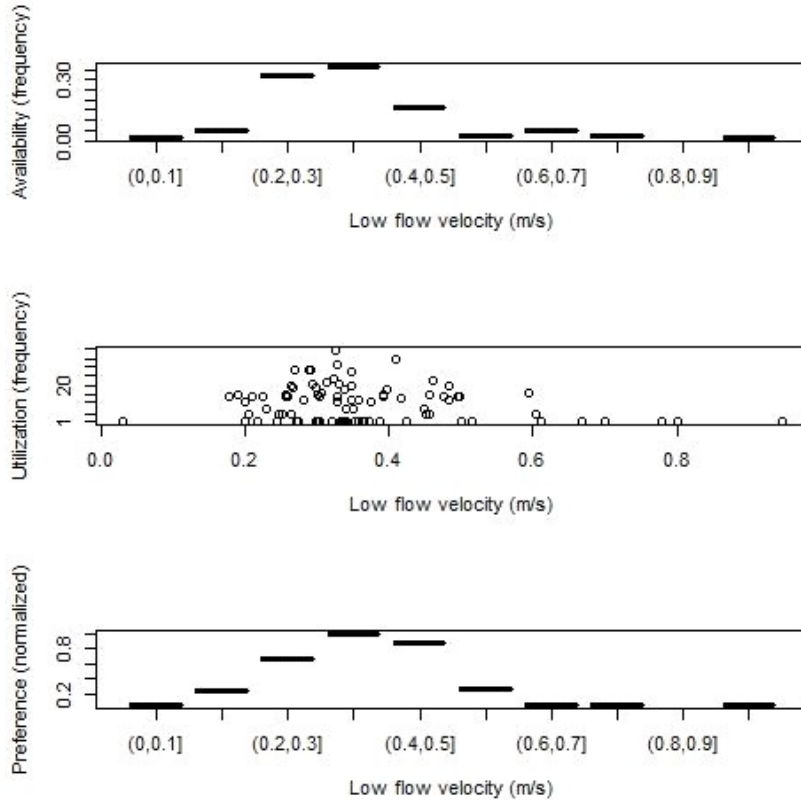


Figure 29 – Habitat availability (up), individuals utilization (middle) and habitat preference (bottom) for Q20 flow velocity.

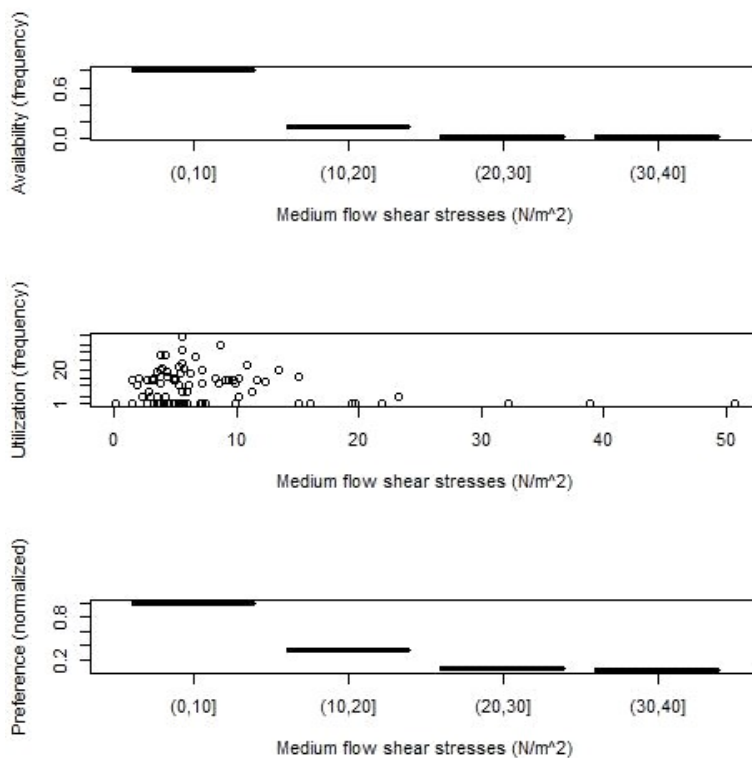


Figure 30 – Habitat availability (up), individuals utilization (middle) and habitat preference (bottom) for Q50 shear stresses.

6.3 Habitat modeling at the catchment scale

The habitat curves derived in the previous section are an indication of the clear preference of FPM for specific physical habitat conditions but can't be used in modeling the potential habitat because they do not respond to quality requirements for predictive models (in specific, no uncertainty is assessed and no validation of the curves can be performed with a single dataset). Therefore, species distribution models were used to determine the potential FPM habitat in a solid modeling framework.

Two already published datasets (Yung et al., 2013 and Huemer et al., 2016) for the Waldaist population were used to fit the Species Distribution Models (SDMs). Abundance data were snapped to the closest raster cell centroid of the environmental layers and transformed to presence data, thus resulting in 69 known positions used to fit the models. Presence-only data from the dataset were used, aiming at disentangling realized and potential distributions (Marger et al., 2013).

The biomod modeling procedure employs several algorithms and provides an ensemble forecasting to reduce uncertainties related with the choice of the modeling algorithm (consensus model, Thuiller et al., 2009) and to improve the robustness of the forecast (Araujo and New, 2007). A consensus model was created for FPM based on a generalized linear model (GLM), a generalized additive model (GAM), a generalized boosting model (GBM) and a maximum entropy model (MaxEnt) for a total of 40 fitted models.

Each algorithm used a high number of pseudo absences (500), and a 10-fold cross validation following the indications by Barbet-Massin et al. (2012). The input dataset was split into a training set (70%) and a testing set (30%). Because of the small size of the dataset used to train the SDMs, only hydraulic predictors and riparian land use predictors were used to fit the models (Jähnig et al., 2012).

The final consensus results from the weighted average of the single algorithm models (Marmion 2009) by multiplying the AUC (area under the receiving operating characteristic curve) scores with a decay of 1.6. The models performances were evaluated with the AUC metric. AUC received strong criticisms when applied to presence-only data (Lobo et al., 2010), therefore also TSS (true skill



statistics) metrics are reported, that are not affected by prevalence (Allouche, 2006). A threshold that balances omission and commission errors was applied to discriminate the output habitat suitability index (HSI) between suitable and unsuitable values.

Relative variable importance in the ensemble model was evaluated by randomly permuting the variable and expressed as the inverse of the correlation between the original model and the permuted one (Araujo, 2010).

6.4 Connectivity assessment

The overall landscape connectivity was assessed with a slightly modified formulation of the probability of connectivity index (PC, Saura and Pascual-Hortal, 2007), defined as the probability that two habitat patches randomly placed in the landscape are reachable from each other, given a set of n patches and p_{ij} connections among them:

$$PC = \frac{\sum_{i=1}^n \sum_{j=1}^n a_i a_j p_{ij}^*}{A^2}$$

Where a_i and a_j are the habitat quality values of the two habitat patches (here the raster cells HSI values) and A is the total area of the landscape. p_{ij}^* is the probability of colonization, from an exponential dispersal kernel as defined by Visconti and Elkin, 2009:

$$p_{ij}^* = \exp(-\alpha d_{ij})$$

Where α is the inverse of the species dispersal distance and d_{ij} is the river-network distance between the patches i and j over the shortest path. Following the indications in Höjesjö et al. (2014) and Young et al. (2010), the dispersal distance was set to 1 km accordingly to brown trout juveniles movement abilities. The relative importance of each patch is calculated as relative connectivity drop as the patch is removed:

$$dPC = \frac{(PC - PC')}{PC} \times 100$$

Where PC' is the PC index after the removal of the patch of interest. A threshold equivalent to the dPC value that each habitat patch would have if every habitat patch would equally contribute to the landscape connectivity was used to discriminate between important sites for connectivity and non-important sites for connectivity. Raster cells were used as habitat patches.

6.5 Freshwater Pearl Mussel habitat niche

The ensemble habitat model showed good capacities in discriminating potentially suitable habitat (AUC = 0.88, TSS = 0.61, Sensitivity = 0.87, Specificity = 0.73). The most important retained variables are high flow shear stresses, riparian forest fraction and flow velocity during low flows. Ensemble partial dependence plots are showing an increasing suitability with the increase of riparian land use occupied by forest. Shear stresses and flow velocity dependences have an optimum value around respectively 25 Pa and 25 cm s⁻¹. The ensemble model predicts 34% of the stream network area to be potentially suitable for FPM. No significant differences in predictors values were detected between the sites where FPM is predicted to occur and sites where it has been sampled (Table 15, Mann-Whitney U test non-significant for all predictors).

Species occurrence was higher in sites with low shear stresses, intermediate flow velocities and medium-high riparian land use.

FPM was predicted to occur in sites with low shear stresses during high flow, with an optimum of 15 Pa and marginal suitability above 50 Pa. Shear stresses have been recognized as an important factor limiting freshwater mussels richness and abundance (Allen and Vaughn, 2010), being related with substrate stability. Riparian forest cover shows a marked preference of FPM for river sections whose banks are occupied by vegetation, accordingly to Wilson et al. (2011). The presence of riparian forest is an indication that a section of river was not disturbed or modified, for example by



banks re-sectioning or channel dredging. Flow velocity during low flow shows an optimum relationship, low values being related with nutrients provisioning (Quinlan, 2015).

Table 15 – FPM habitat niche identification

	Sampling sites (\pm SD)	Predicted occurrence (\pm SD)	Study area
Shear stresses (Pa) during high flow	15.9 (\pm 10.9)	15.9 (\pm 8.2)	0-455.1
Flow velocity ($m\ s^{-1}$) during low flow	0.27 (\pm 0.10)	0.27 (\pm 0.08)	0–3.20
Forested riparian land use (%)	0.67 (\pm 0.33)	0.70 (\pm 0.30)	0-1

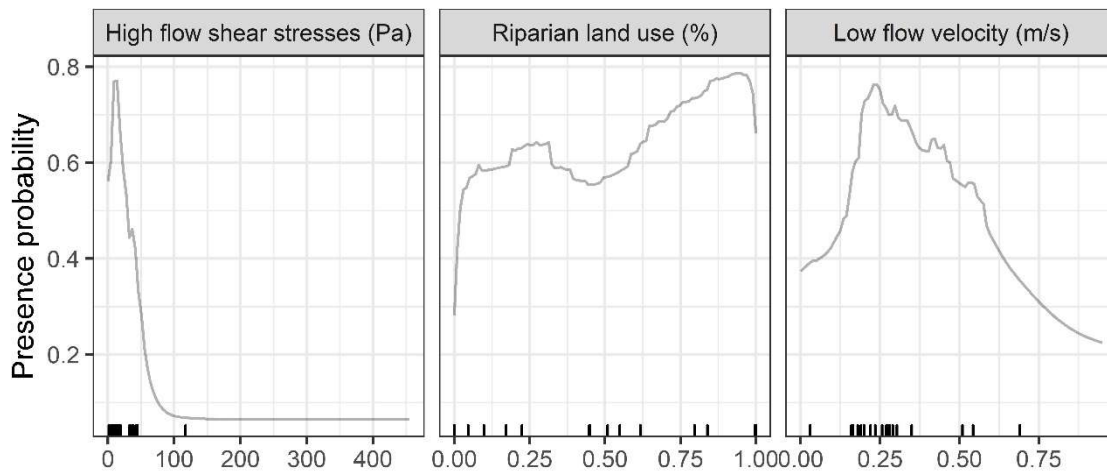


Figure 31 – Response of FPM to the ecological gradients

7. BASELINE CONDITIONS

The habitat model and the siltation model allow predicting the spatial distribution of the potential habitat for FPM and the extent of the siltation for the whole Aist catchment by projecting the model on the environmental predictors.

The siltation model predicts the fine sand accumulation status to be more marked in all the tributaries. The habitat model predicts the potential habitat for FPM to be mostly located in the main stems of Feldaist and Waldaist (Fig. 33).

The results of the model are reported also in Fig. 34, 35 and 36.

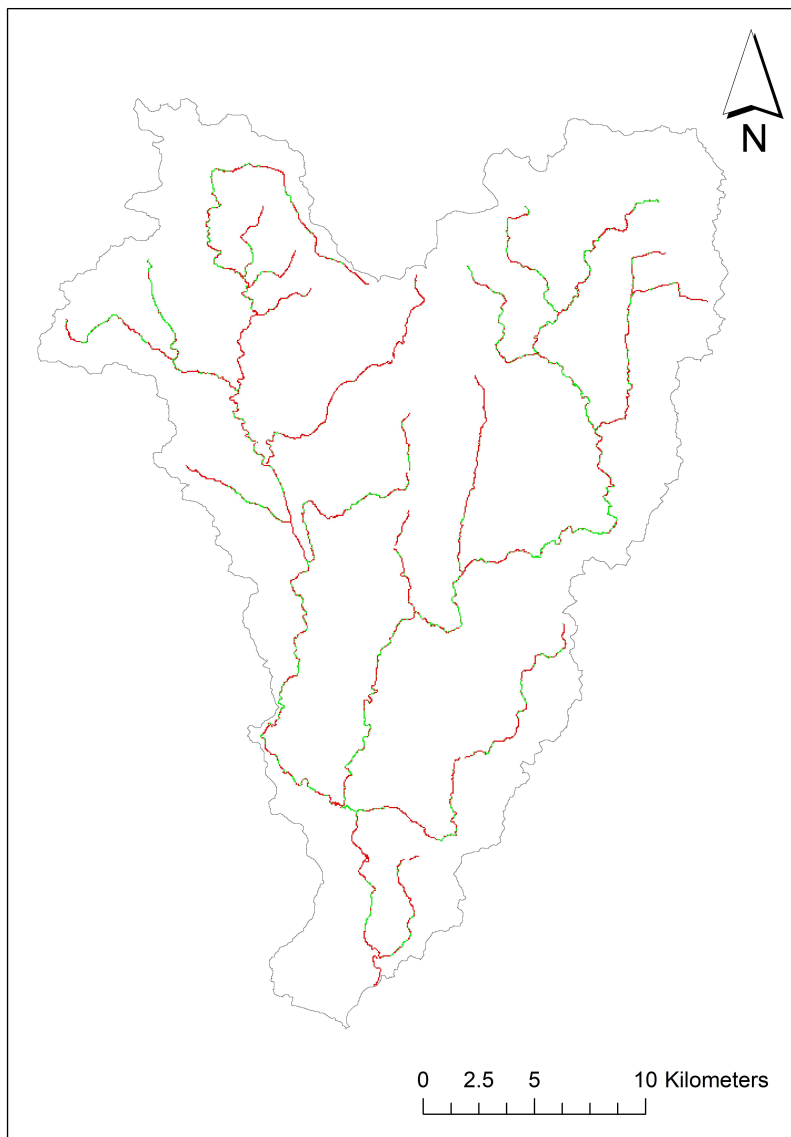


Figure 32 – Predicted boolean habitat suitability for FPM. Red stretches are unsuitable, gree stretches are suitable. The binary classification was based upon the identification of



7.1 Siltation status

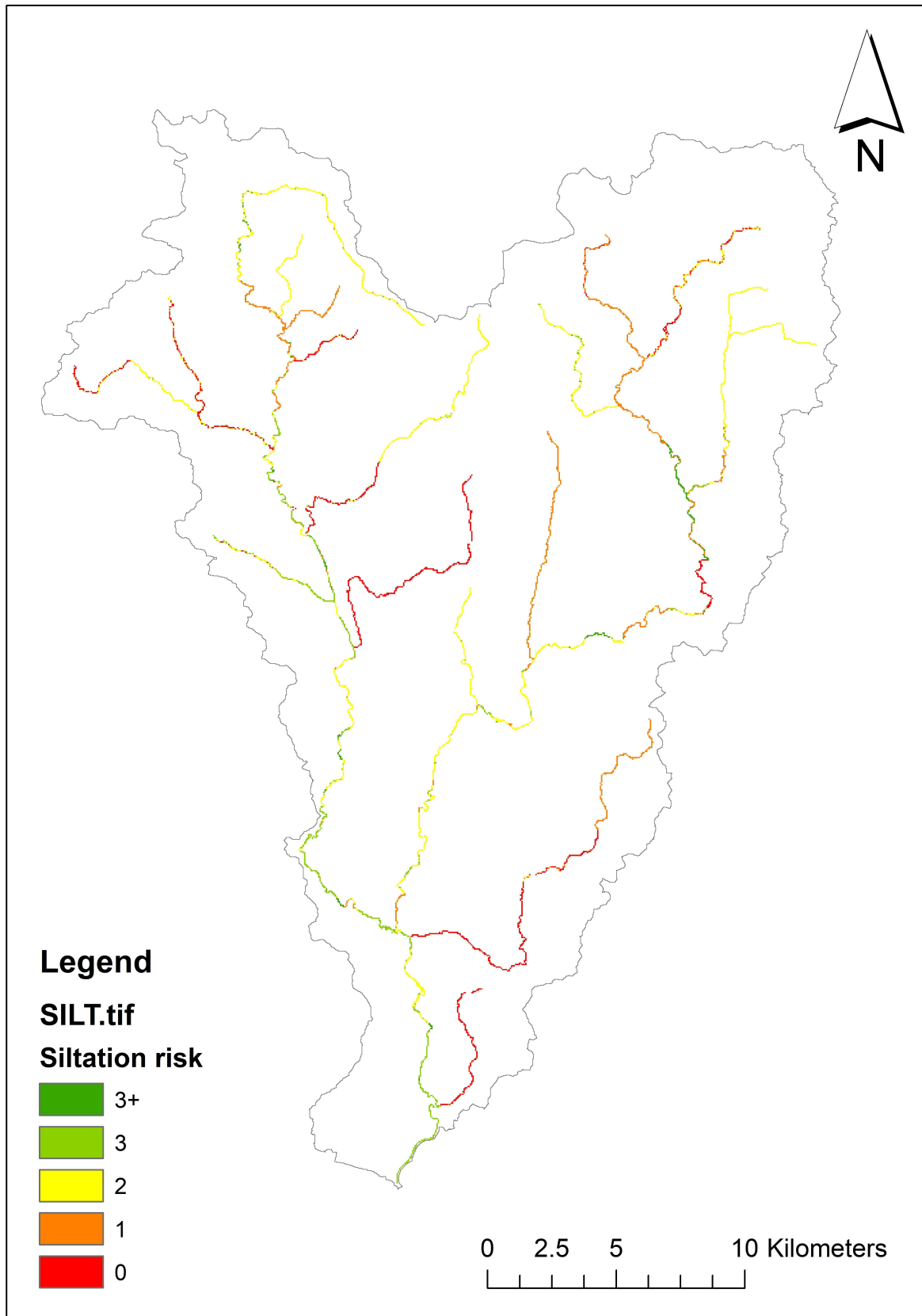


Figure 33 - Random forest model output for siltation

7.2 Habitat status

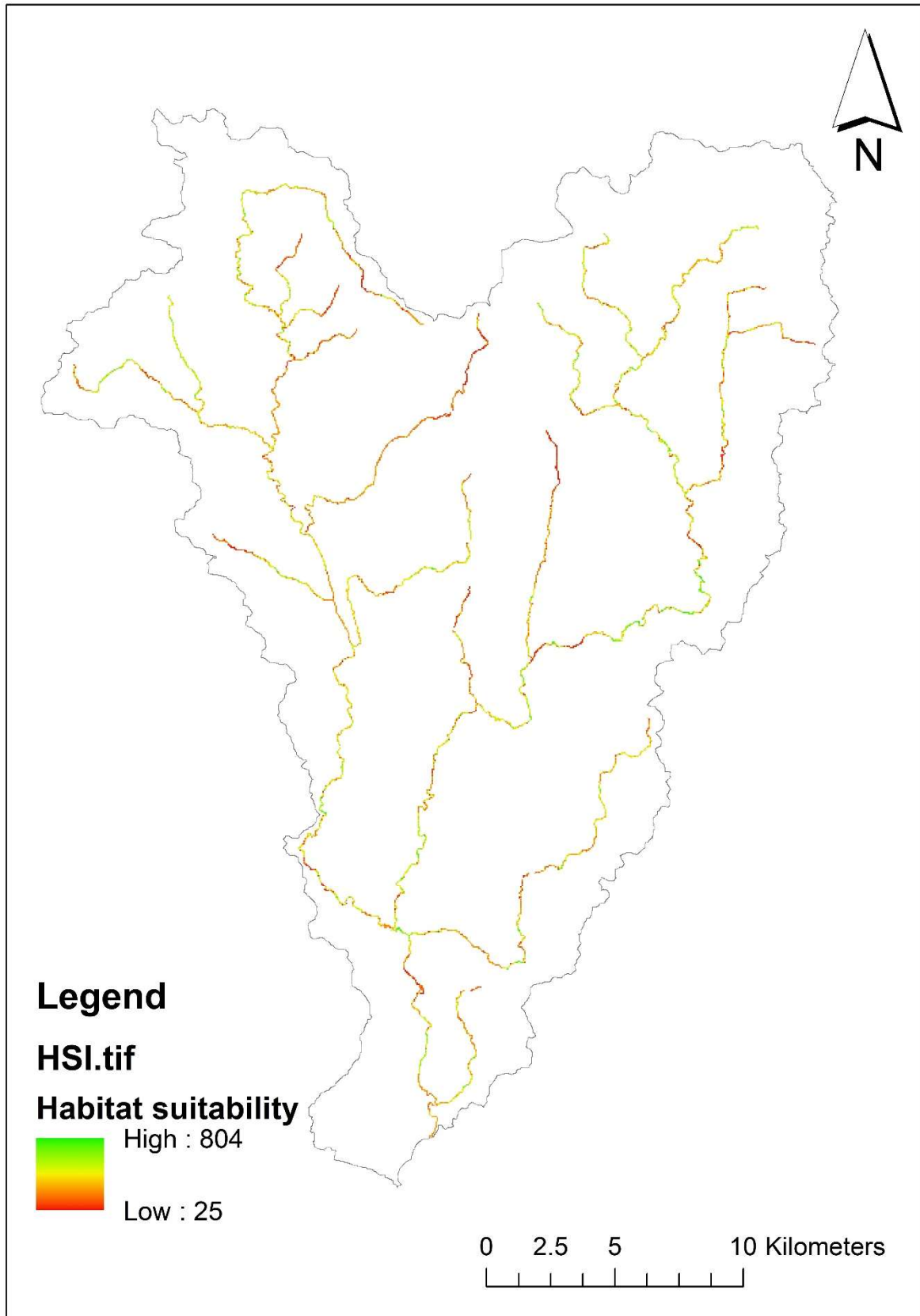


Figure 34 – Habitat model result. Note: habitat suitability is expressed as fractions of 1000.

7.3 Connectivity

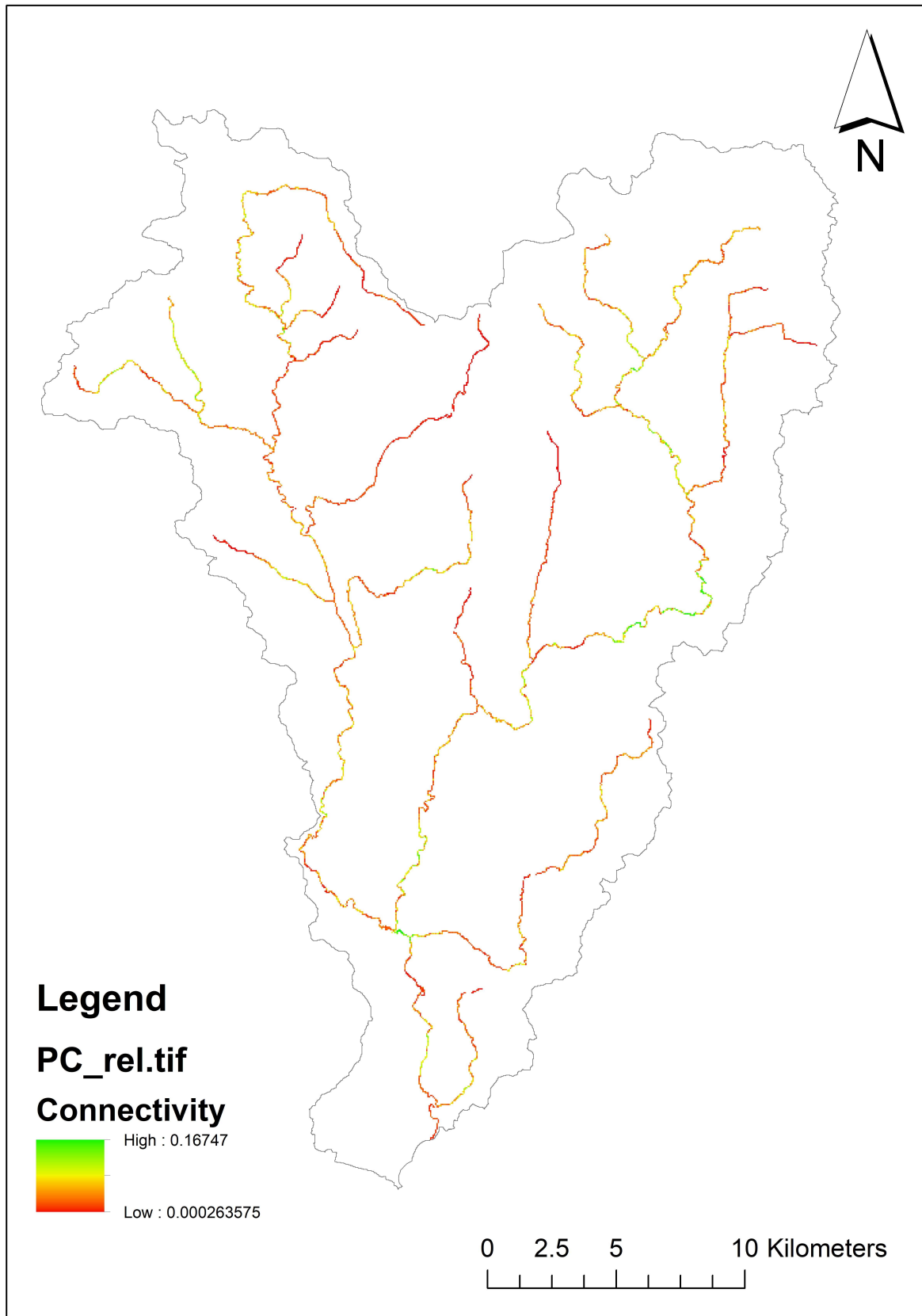


Figure 35 – Connectivity assessment of the Aist catchment. Since connectivity is assessed as relative drop, units are adimensional



7.4 Siltation effects on habitat availability

The overlay between the siltation risk, the habitat suitability and the connectivity drop maps allows assessing the patterns of spatial interactions (Fig. 37). The mean habitat suitability for each siltation class is always significantly below the suitability threshold, i.e. there is no clear evidence on the occupancy preference of siltation on highly suitable habitats. Only the sites that are falling within the highest siltation risk class (3+) are those that are contributing significantly to the landscape connectivity (Wilcox test, $p < 0.001$), whereas all the lower siltation risk class are those that are contributing less to the overall connectivity.

Note: in this report the terms siltation, fines accumulation and sand accumulations are used as synonyms and refer to accumulations of sediments with a mean diameter between 1 and 10 mm that are resulting from the erosion of the granitic substrate. Refer to Hauer et al., 2015; Leitner et al., 2015; Scheder et al., 2015 for further details on the siltation issue in the region.

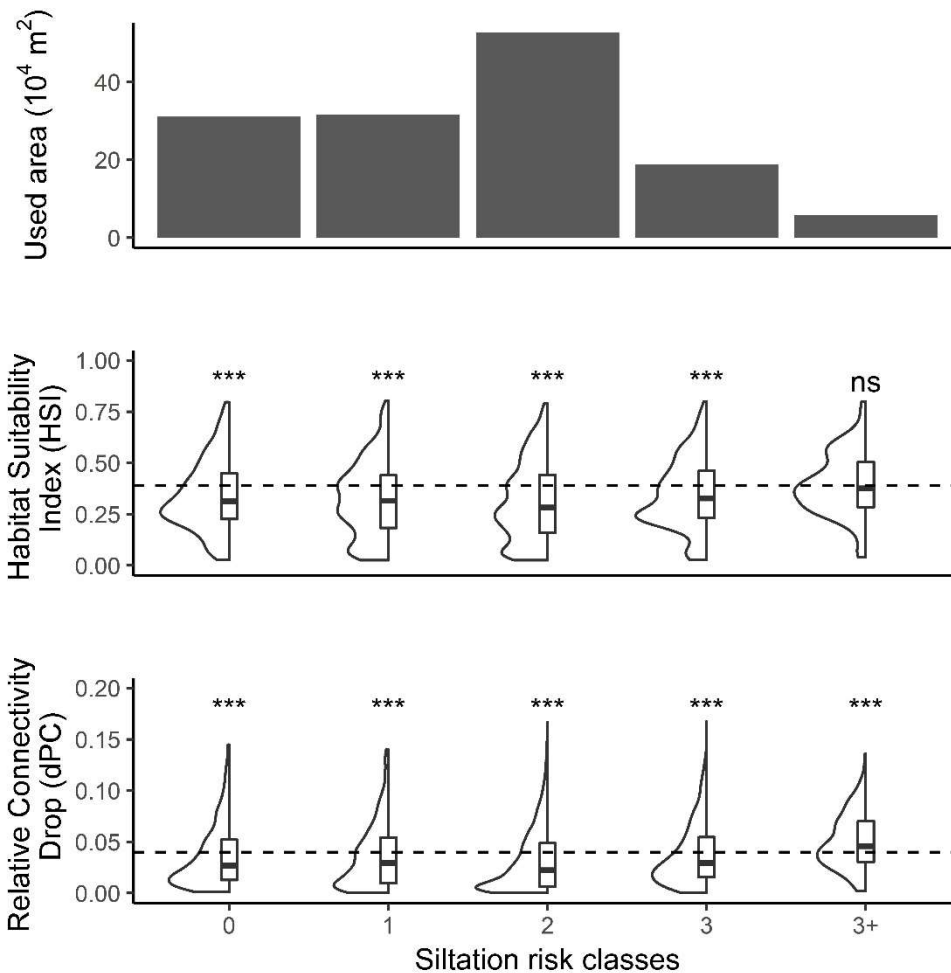


Figure 36 – Impact of siltation on habitat availability and relative connectivity drop. Asterisks are indicating the significance level of Wilcox test. ***: $p < 0.001$; ns: test not significant



7.5 Baseline summary

The simulated siltation shows that the most critically impacted reaches are the main stems of Feldaist and Waldaist.

The species distribution models predict potentially suitable habitat to be evenly distributed in the catchment, with a dominance of potentially suitable sites in the main stems of Feldaist and Waldaist

The connectivity assessment reveals that potentially suitable habitats in the Fedaist are fragmented and practically unavailable for colonization because they are surrounded by bigger portions of the riverine landscape that are not suitable. On the contrary the Waldaist offers habitats that are well connected with each other and therefore more suitable for recolonization.

These well-connected habitats are also the ones that are more prone to fine sand accumulation.



8. NSWRMS TESTING IN THE AIST CATCHMENT

Natural small water retention measures were tested in the dynamic models for the Aist catchment. The aims of the implementations were:

- To test the feasibility of measures implementation in the models framework,
- To test the sensitivity of the models framework to the implementation of measures
- To test the maximum potential improvement that is possible to obtain from the implementation of some measures
- To test the potential synergies of combined implementation of NSWRMs
- To rank measures based on their maximum potential benefit to in-stream sand accumulation risk and habitat availability

8.1 Methodology

The methodology for measures implementation and the propagation of their effects is as follows:

1. Measures were implemented in SWAT, following the guidelines from Neitsch et al (2011), or according to expert-based parametrization
2. The reach and sub-catchment level outputs (output.rch and output.sub) were extracted from SWAT output files
3. Indicators of hydrological alteration, sediment loads indicators and flow percentiles were extracted from the output files and used to create scenario-based predictors.
4. Predictors were put into the siltation model and the habitat model and scenarios were generated.

Accordingly to the concept plan, tree types of measures were implemented, that tackle both the issue of water retention and sediment cycle balance:

1. Stream hydromorphological improvement (HYDROMORPHO);
2. Vegetated buffer strips (BUFFER);
3. Sediment retention ponds (PONDS_25);
4. A combined scenario with vegetated buffer strips and hydromorphological improvement (HYDROMORPHO_BUFFER)

Those measures correspond to the following coes in the catalogue of measures:

- Stream hydromorphological improvement: BPRC - Natural channels and best practices of river channels maintenance (e.g. riverbed material re-naturalization, stream bed re-naturalization, natural bank stabilization, elimination of riverbank stabilization...);
- Small sediment retention ponds: BPDA - Best practices on drained areas: installation of small sediment retention ponds (located in-stream and off-stream);
- Vegetated buffer strips: A02 (buffer strips and hedges).

The measures were implemented as follows.

- Buffer strips were parametrized in the .ops input file, modifying the VFSRATIO and VFSCON parameters. VFSRATIO is an indication of implementation magnitude (ratio of the area of the buffer strip and the area of the field); VFSCON is a reduction factor accounting for flow that may bypass the buffer strip.
- Hydromorphological improvement was parametrized by increasing channel roughness, e.g. to simulate the re-meandering or the improvement of the riverbed roughness values. CH_N2 was increased by 0.05.



- Ponds were simulated in the .pnd input file, by assigning a volume of 200 m³/ha (total volume was calculated based on the sub-catchment area) and a draining area equal to 25% of the potential sub-catchment drainable area.

The meaning of the parameters in the SWAT model is explained in detail in Neitsch et al. (2012).

The rationale behind this test is to allow for assessing the maximum potential improvement following the uniform, catchment-scale implementation of some measures to allow for a more solid decision making process concerning the exact identification of measures locations. The combined scenario consisted in the simultaneous implementation of hydromorphological improvements (that are modifying only hydraulics) and buffer strips (that are affecting only sediment transport), so that it's possible to observe the combined effects.



8.2 Effects on hydrology and sediment generation

The first results from the implementation of measures concern the hydrological and sedimentological response of the catchment (Fig. 38).

- Buffer strips do not affect the hydrological component of the SWAT model, therefore their impact is not visible in the selected indicators of hydrological alteration.
- Hydromorphological alterations do not show a clear pattern in changing duration of high and low flows, in the frequency of low flows and in the timing of flood events. On the contrary, hydromorphological improvements are reducing the frequency of high flows and the flow rate of change.
- Ponds are reducing the duration and the frequency of high flows and increasing the duration of low flows and the flow rate of change, while no clear pattern is visible for the frequency of low flows and for the floods timing.

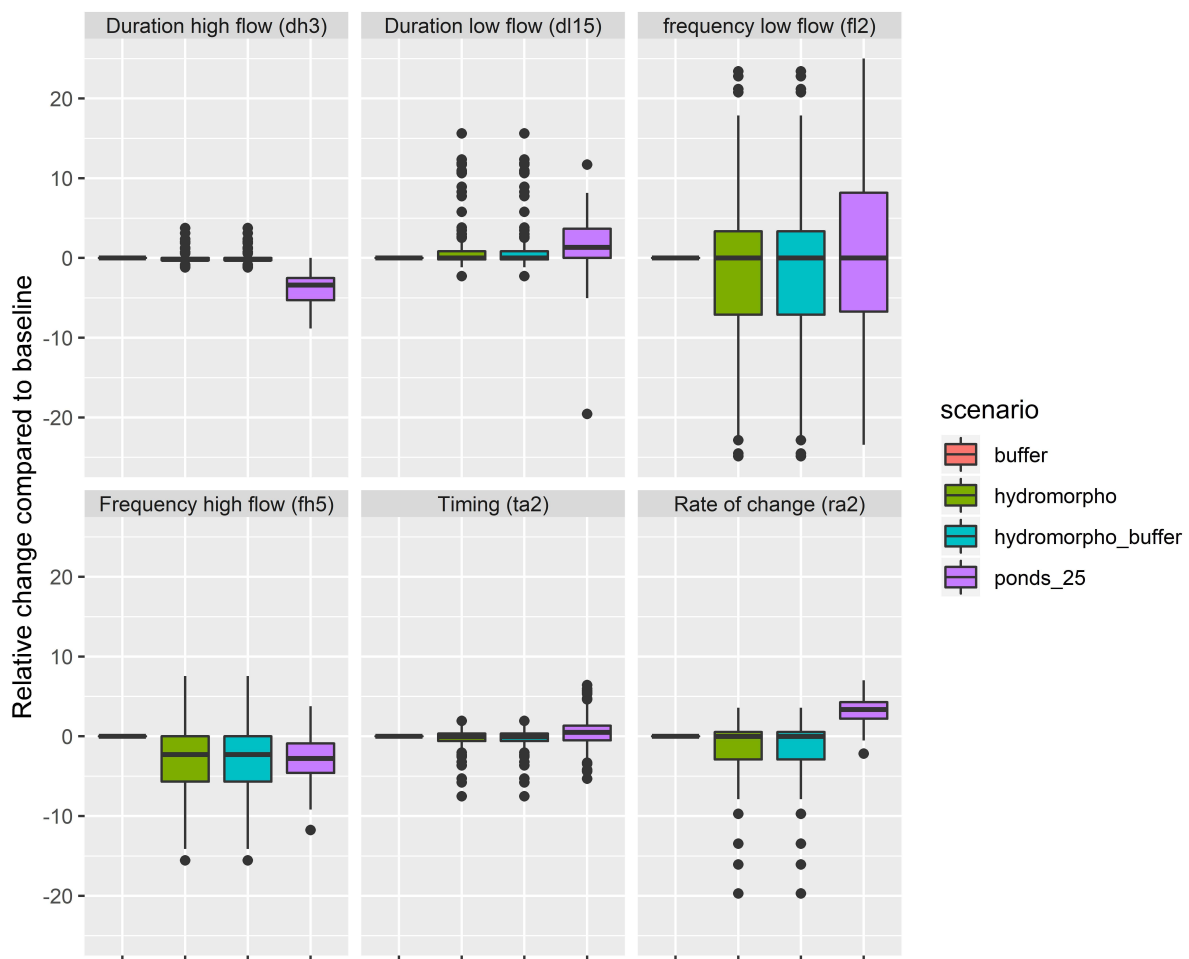


Figure 37 – Effects of NSWRMs implementation on hydrological response of the Aist catchment. The boxplots represent the variability between subbasins (n=103)



Concerning sediment loads response, hydromorphological alterations are not affecting the sediment generation from upstream. Buffer strips are able to reduce up to 50% of the sediment loads, while ponds are providing a lower reduction of sediment loads, approximately 20% (Fig. 39).

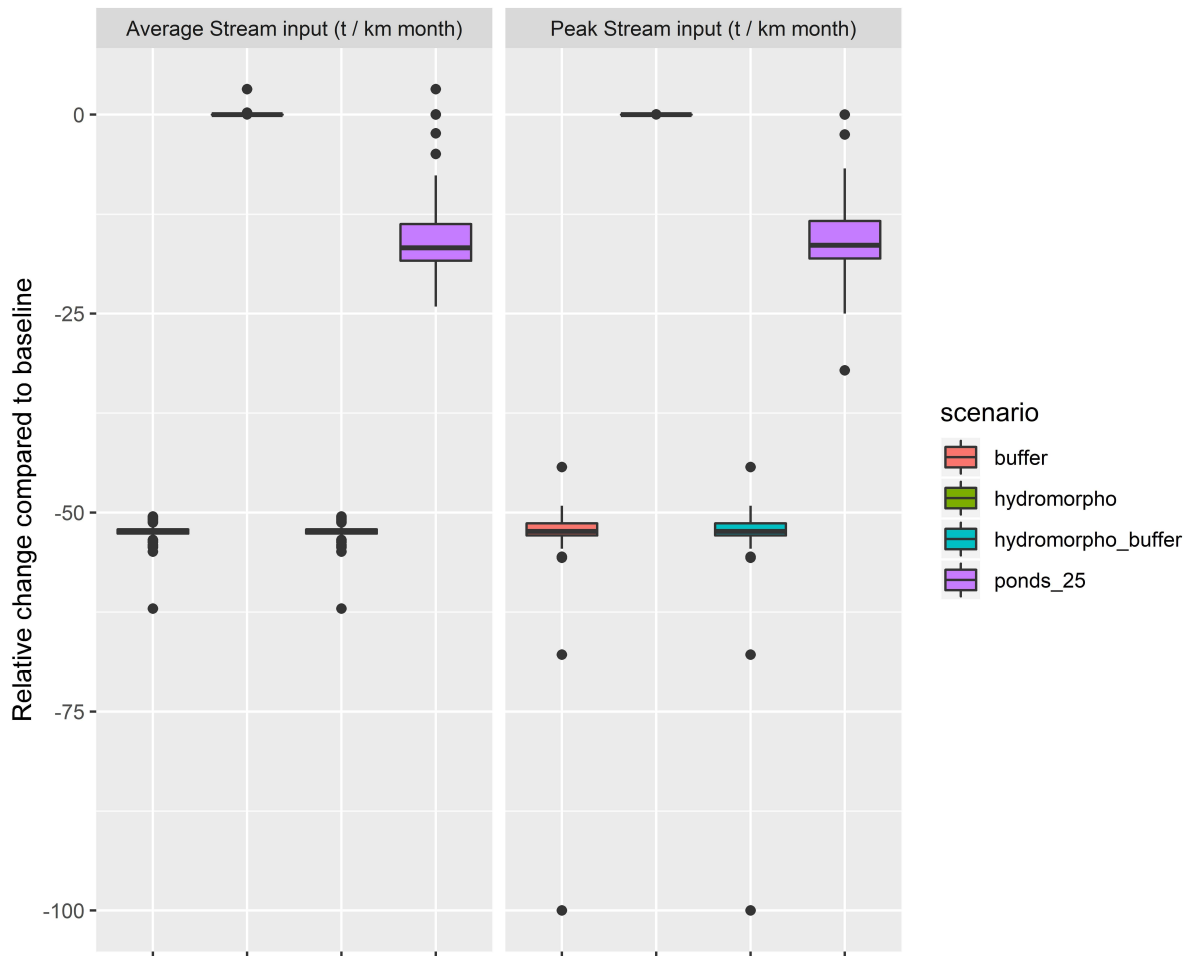


Figure 38 - Effects of NSWRMs implementation on sediment response of the Aist catchment. The boxplots represent the variability between subbasins (n=103)



8.3 Effects on hydraulics

The hydrological effects are then propagated in the hydraulic model, leading to changes in the local hydraulics. Buffer strips are not affecting local hydraulics. Ponds are reducing both high flow and low flows predictors for flow velocity, shear stresses and stream power. Hydromorphological improvements do not show clear patterns for high flow predictors and for flow velocity, increasing slightly shear stresses and stream power during low flows (Fig. 40).

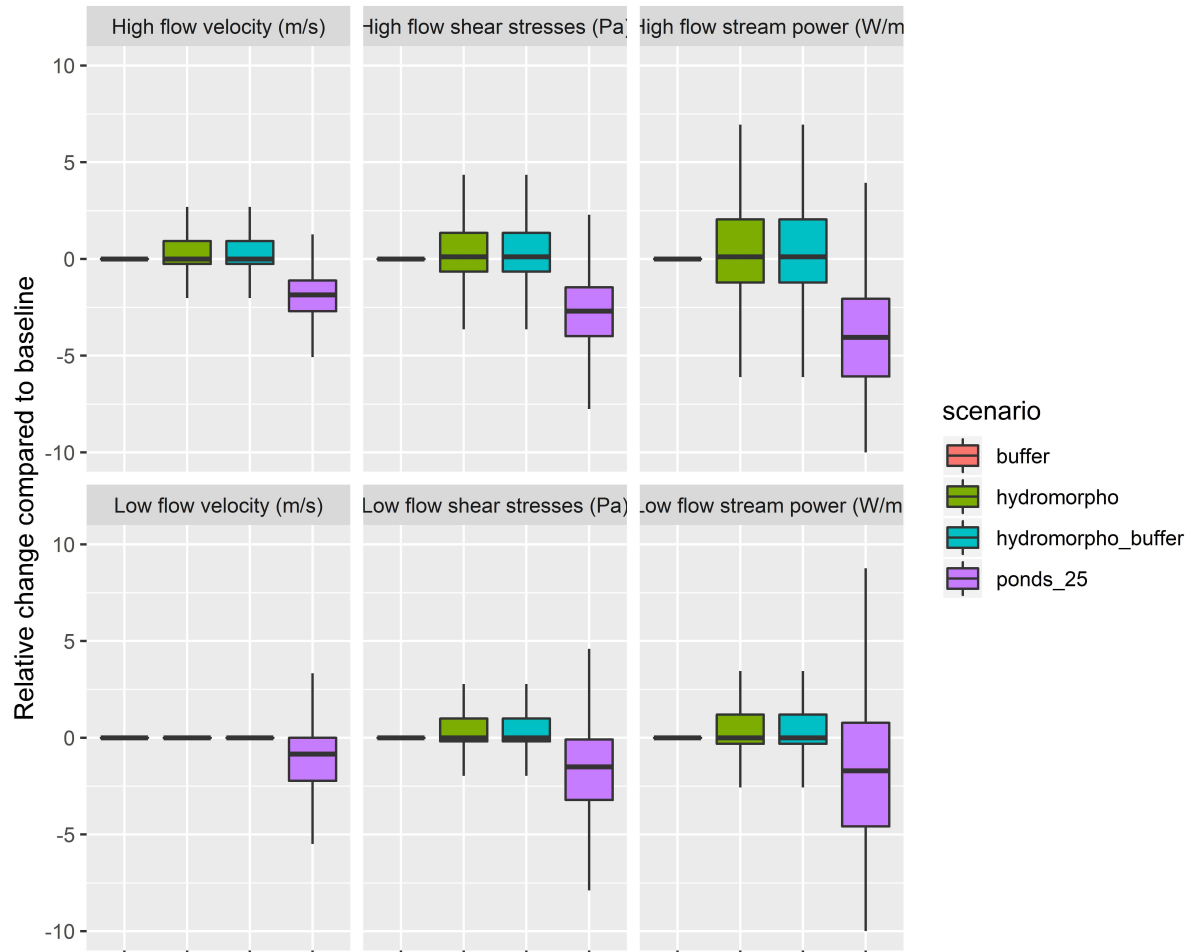


Figure 39 - Effects of NSWORMs implementation on hydraulic response of the Aist catchment. The boxplots represent the variability between subbasins (n=103)



8.4 Effects on sand accumulation

Finally, measures effects are propagated in the Random Forest model to assess changes of in-stream sand accumulations. All the proposed measures are reducing the amount of sites affected by heavy siltation (class 3+), but only buffer strips are effective in creating new sites for the low risk class (class 0) (Fig. 41).

The combined implementation of buffer strips and hydromorphological improvements allowed to achieve the highest reduction of sites under the highest risk class and at the same time creating new sites that are free of sand (or occupied a little)

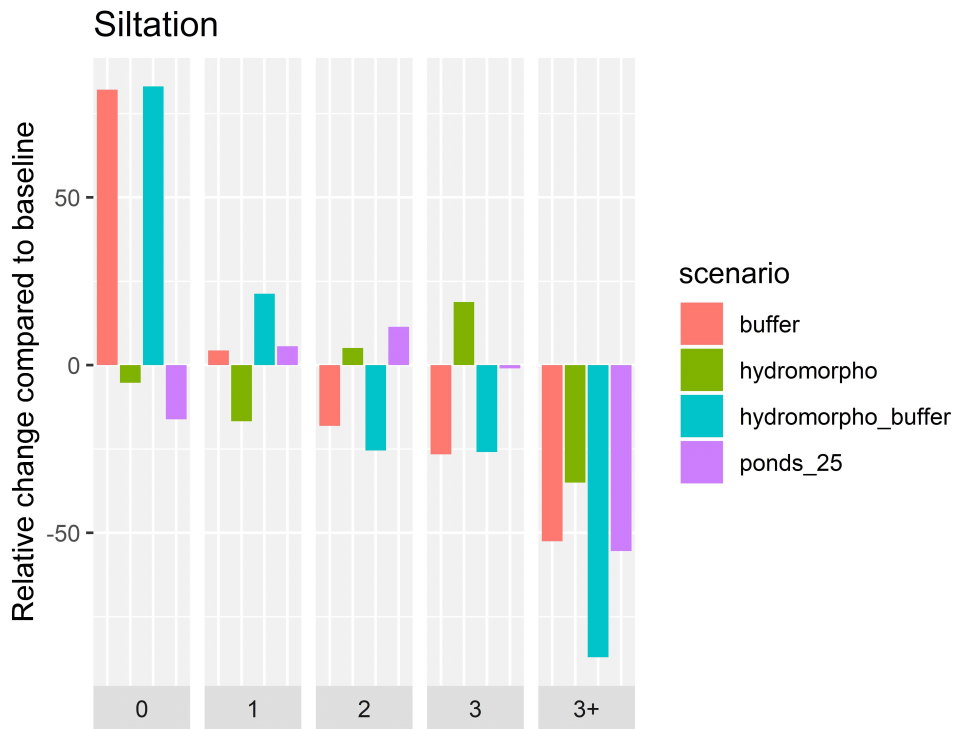


Figure 40 - Effects of NSWRRMs implementation on siltation risk response of the Aist catchment. The response has been aggregated in terms of relative changes in number of siltation risk classes



8.5 Effect on habitat availability

Changes in local hydraulics affect also the potential habitat of FPM. Fig.42 shows that the effect is always positive, and Fig. 43 shows that a significant improvement in habitat is observed also when siltation is accounted and sites prone to siltation are removed from the analysis.

However, no clear indication for choosing a specific measure for the habitat can be obtained from the modeling exercise.

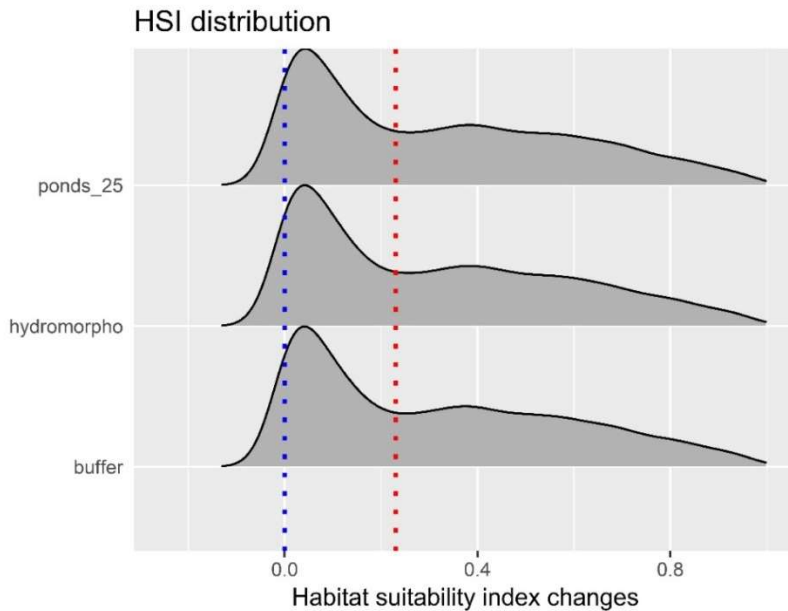


Figure 41 - Effects of NSWORMs implementation on Habitat availability of the Aist catchment. The plot represent changes in habitat suitability indices.

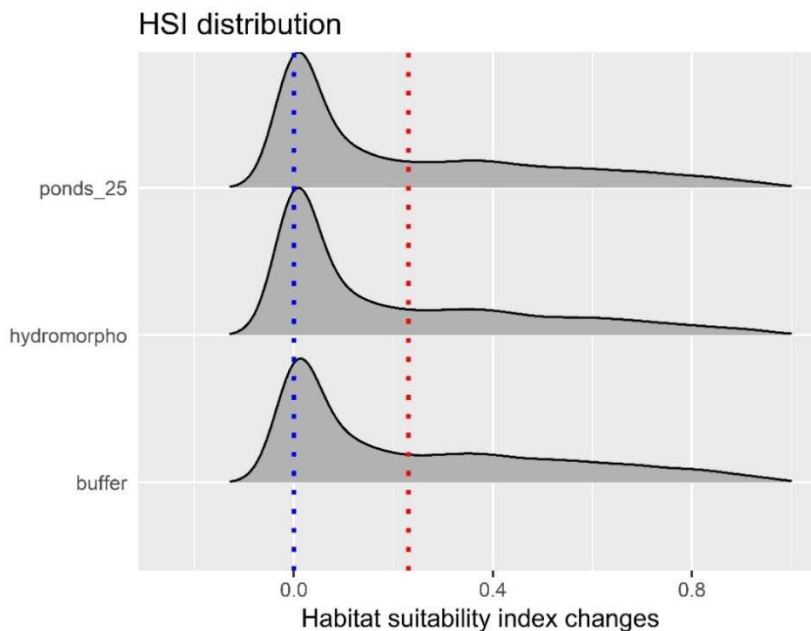


Figure 42 - Effects of NSWORMs implementation on habitat availability of the Aist catchment. The plot represent changes in habitat suitability indices. The response is now lower because sites prone to siltation risk have been removed from the analysis.

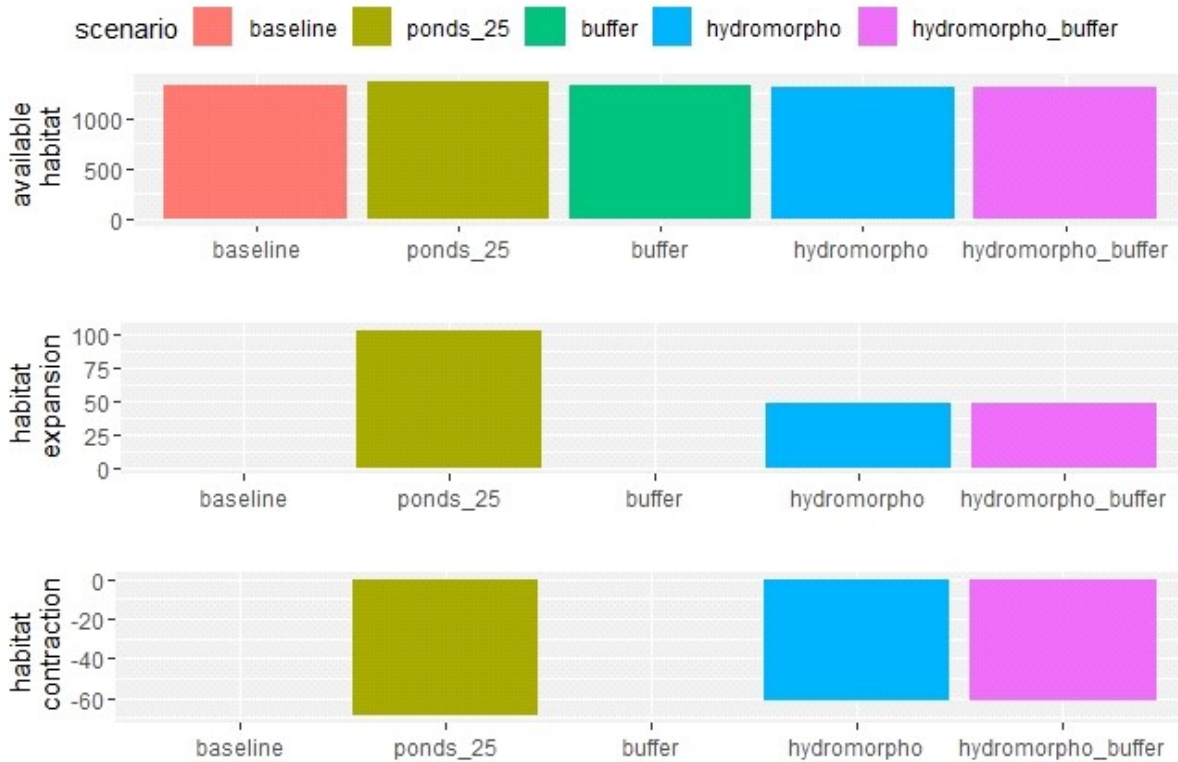


Figure 43 – Absolute habitat change and ranges expansion and contraction after the implementation of measures. Units on the y axes are raster cells, corresponding to 250 m² (50 m resolution)

Also, when considering the boolean habitat thresholding (i.e., the habitat suitability index is split in two classes, suitable and unsuitable), the relative change in habitat following the implementation of measures are limited, with positive values for sediment ponds, no changes for buffer strips and even worsening for hydromorphological improvements.



8.6 NSWORMs testing conclusions

Among the tested measures, buffer strips were affecting only the sediment loads and were the only measures for which both a reduction of sites with high siltation risk (class 3+) and an increase in sites with low silt accumulation (class 0) was observed. The combined implementation of buffer strips and hydromorphological improvements allowed improving the stream conditions regarding all the sand classes and was more effective than the two measures considered alone. Therefore the exploration of possible alternatives for NSWORMs in this modeling framework should focus on the simultaneous implementation of several types of measures at the same time.

Both hydromorphological improvements and ponds are able to reduce the amount of high risk sites at the expense of decreasing the amount of sites that are in good conditions. The impact of the measures on habitat availability is comparable, therefore an accurate planning process should focus on the reduction of sand accumulations.

The results are a useful basis for a further NSWORMs planning in the catchment in more detail (spatially distributed implementation).



9. CONCLUSIONS

This report examined the possibility to implement an ecohydrological modeling cascade to link hydrology, hydraulics, sediments production, reach scale fines accumulation and habitat availability in a process-based framework. The developed cascade was used to test the potential impact of natural small water retention measures (NSWRMs) on stream siltation status and habitat availability.

The simulated siltation shows that the most impacted reaches are the main stems of Feldaist and Waldaist, with a high proportion of sites occupied by accumulations that are movable even during low flow in the Feldaist. The species distribution models predict potentially suitable habitat to be evenly distributed in the catchment, with a dominance of potentially suitable sites in the main stems of Feldaist and Waldaist. Potentially suitable habitats are showing low shear stresses during high flow, high proportion of forest cover in the riparian area and medium flow velocities during low flows.

The connectivity assessment reveals that potentially suitable habitats in the Fedaist are fragmented and practically unavailable for colonization because they are surrounded by bigger portions of the riverine landscape that are not suitable. On the contrary the Waldaist offers habitats that are well connected with each other and therefore more suitable for recolonization.

These well-connected habitats are also the ones that are more prone to fine sand accumulation.

NSWRMs are offering a potential mitigation tool for fine sediment accumulations, with buffer strips being more effective in reducing the sediment loads from the catchment to the stream, therefore being able to free some sites from siltation. No clear preference concerning critical accumulation classes was detected in the test since all the measures were equally good in reducing the amount of sites prone to accumulations.

All the proposed measures provided potentially new habitat, no clear preference for a set of measures was detected.



10. REFERENCES

- Abbaspour, K. C. (2013). SWAT-CUP 2012. SWAT Calibration and Uncertainty Program—A User Manual.
- Allen, D. C., & Vaughn, C. C. (2010). Complex hydraulic and substrate variables limit freshwater mussel species richness and abundance. *Journal of the North American Benthological Society*, 29(2), 383-394.
- Allen, D. C., & Vaughn, C. C. (2010). Complex hydraulic and substrate variables limit freshwater mussel species richness and abundance. *Journal of the North American Benthological Society*, 29(2), 383-394.
- Allouche, O., Tsoar, A., & Kadmon, R. (2006). Assessing the accuracy of species distribution models: prevalence, kappa and the true skill statistic (TSS). *Journal of applied ecology*, 43(6), 1223-1232.
- Araújo, M. B., & New, M. (2007). Ensemble forecasting of species distributions. *Trends in ecology & evolution*, 22(1), 42-47.
- Arnold, J. G., Moriasi, D. N., Gassman, P. W., Abbaspour, K. C., White, M. J., Srinivasan, R., ... & Kannan, N. (2012). SWAT: Model use, calibration, and validation. *Transactions of the ASABE*, 55(4), 1491-1508.
- Barbet-Massin, M., Jiguet, F., Albert, C. H., & Thuiller, W. (2012). Selecting pseudo-absences for species distribution models: how, where and how many?. *Methods in ecology and evolution*, 3(2), 327-338.
- Bartier, P. M., & Keller, C. P. (1996). Multivariate interpolation to incorporate thematic surface data using inverse distance weighting (IDW). *Computers & Geosciences*, 22(7), 795-799.
- BMLFUW (Hrsg.)(2010): Leitfaden zur hydromorphologischen Zustandserhebung von Fließgewässern, Wien, 71 S. + Anhang.
- BMLFUW, 2019. Integriertes Verwaltung- und Kontrollsystem, Bundesministerium für Land- und Forstwirtschaft, Umwelt und Wasserwirtschaft, Wien. Accessed from www.data.gv.at
- Breiman, L. (2001). Random forests. *Machine learning*, 45(1), 5-32.
- Buffington, J. M., & Montgomery, D. R. (1997). A systematic analysis of eight decades of incipient motion studies, with special reference to gravel-bedded rivers. *Water Resources Research*, 33(8), 1993-2029.
- Bundesministerium für Land- und Forstwirtschaft, Umwelt und Wasserwirtschaft (BMLFUW), 2017. Nationaler Gewässerbewirtschaftungsplan 2015. Wien, 2017. Bolla Pittaluga, M., Luchi, R., Seminara, G., 2014. On the equilibrium profile of river beds. *J. Geophys. Res. Earth Surf.* 119, 317–332. <https://doi.org/10.1002/2013JF002806>
- DORIS, 2017. 10m resolution DEM. Digitales Oberösterreichisches Raum-Informationssystem, Linz. Accessed from <https://www.doris.at>
- Doyle, M. W., Shields, D., Boyd, K. F., Skidmore, P. B., & Dominick, D. (2007). Channel-forming discharge selection in river restoration design. *Journal of Hydraulic Engineering*, 133(7), 831-837.
- Gassman, P. W., Reyes, M. R., Green, C. H., & Arnold, J. G. (2007). The soil and water assessment tool: historical development, applications, and future research directions. *Transactions of the ASABE*, 50(4), 1211-1250.
- GBA, 2019. Geologische Bundesanstalt, Bundesministerium für Bildung, Wissenschaft und Forschung, Wien. Accessed from <https://www.geologie.ac.at>
- Gomez, B., Coleman, S.E., Sy, V.W.K., Peacock, D.H., Kent, M., 2007. Channel change, bankfull and effective discharges on a vertically accreting, meandering, gravel-bed river. *Earth Surf. Process. Landforms* 32, 770–785. <https://doi.org/10.1002/esp.1424>



- Gupta, H. V., Kling, H., Yilmaz, K. K., & Martinez, G. F. (2009). Decomposition of the mean squared error and NSE performance criteria: Implications for improving hydrological modelling. *Journal of Hydrology*, 377(1-2), 80-91.
- Haddadchi, A., Booker, D. J., & Measures, R. J. (2018). Predicting river bed substrate cover proportions across New Zealand. *Catena*, 163, 130-146.
- Hastie, L. C., Boon, P. J., & Young, M. R. (2000). Physical microhabitat requirements of freshwater pearl mussels, *Margaritifera margaritifera* (L.). *Hydrobiologia*, 429(1-3), 59-71.
- Hauer, C. (2015). Review of hydro-morphological management criteria on a river basin scale for preservation and restoration of freshwater pearl mussel habitats. *Limnologica*, 50, 40-53.
- Hauer, C., 2015. Review of hydro-morphological management criteria on a river basin scale for preservation and restoration of freshwater pearl mussel habitats. *Limnologica - Ecology and Management of Inland Waters*, The current status and future challenges for the preservation and conservation of freshwater pearl mussel habitats 50, 40–53. <https://doi.org/10.1016/j.limno.2014.11.002>
- Hauer, C., Höfler, S., Dossi, F., Flödl, P., Graf, G., Graf, W., Gstöttenmayr, D., Gumpinger, C., Holzinger, J., Huber, T., Janecek, B., Kloibmüller, A., Leitner, P., Lichtneger, P., Mayer, T., Ottner, F., Riechl, D., Sporka, F., Wagner, B., Habersack, H. (2015): Feststoffmanagement im Mühlviertel und im Bayerischen Wald. Endbericht. Studie im Auftrag des Amtes der Oberösterreichischen Landesregierung, gefördert durch das BMLFUW und das Interreg Programm Bayern – Österreich 2007 - 2013. Wien, 391 S.
- HDLO, 2017. Daily precipitation, maximum/minimum temperatures for 13 weather stations; Daily discharge for 5 gauging stations. Hydrographischer Dienst des Landes Oberösterreich, Linz
- LAWA. (2000). Arbeitskreis Gewässerbewertung - Fließgewässer: Gewässerstrukturgütekartierung in der Bundesrepublik Deutschland: Verfahren für kleine und mittelgroße Fließgewässer. Kulturbuch-Verlag, Schwerin.
- Liggett, J., Cunge, J.A. (1975): Numerical methods of solution of the unsteady flow equations. Unsteady flow in open channels, 159–179.
- LODUWAW, 2017. Bi-weekly water chemistry analysis for 5 gauges. Land Oberösterreich, Direktion Umwelt und Wasserwirtschaft, Abteilung Wasserwirtschaft, Linz
- Marcer, A., Sáez, L., Molowny-Horas, R., Pons, X., & Pino, J. (2013). Using species distribution modelling to disentangle realised versus potential distributions for rare species conservation. *Biological Conservation*, 166, 221-230.
- Miori, S., Repetto, R., Tubino, M., 2006. A one-dimensional model of bifurcations in gravel bed channels with erodible banks. *Water Resour. Res.* 42, W11413. <https://doi.org/10.1029/2006WR004863>
- Moriasi, D. N., Wilson, B. N., Douglas-Mankin, K. R., Arnold, J. G., & Gowda, P. H. (2012). Hydrologic and water quality models: Use, calibration, and validation. *Transactions of the ASABE*, 55(4), 1241-1247
- Saxton K.E., Rawls W.J. . 2006. Soil Water Characteristic Estimates by Texture and Organic Matter for Hydrologic Solutions. *Soil Science Society of Agronomy Journal* 70(5):1569-1578
- Neitsch, S. L., Arnold, J. G., Kiniry, J. R., & Williams, J. R. (2011). Soil and water assessment tool theoretical documentation version 2009. Texas Water Resources Institute.
- Quinlan, E., Gibbins, C., Malcolm, I., Batalla, R., Vericat, D., & Hastie, L. (2015). A review of the physical habitat requirements and research priorities needed to underpin conservation of the endangered freshwater pearl mussel *Margaritifera margaritifera*. *Aquatic Conservation: Marine and Freshwater Ecosystems*, 25(1), 107-124.
- Runkel, R.L., Crawford, C.G., and Cohn, T.A., 2004, Load Estimator (LOADEST): A FORTRAN Program for Estimating Constituent Loads in Streams and Rivers: U.S. Geological Survey Techniques and Methods Book 4, Chapter A5, 69 p.
- Saura, S., & Pascual-Hortal, L. (2007). A new habitat availability index to integrate connectivity in landscape conservation planning: comparison with existing indices and application to a case study. *Landscape and Urban Planning*, 83(2-3), 91-103.



Sieck, L. C., Burges, S. J., & Steiner, M. (2007). Challenges in obtaining reliable measurements of point rainfall. *Water Resources Research*, 43(1).

Strobl, C., Malley, J., & Tutz, G. (2009). An introduction to recursive partitioning: rationale, application, and characteristics of classification and regression trees, bagging, and random forests. *Psychological methods*, 14(4), 323.

Thuiller, W., Lafourcade, B., & Araujo, M. (2010). Presentation manual for BIOMOD. Thuiller W, Lafourcade B, Engler R, Araújo MB (2009) BIOMOD-a platform for ensemble forecasting of species distributions. *Ecography*, 32, 369-373.

Vigiak, Olga, et al. "Modelling sediment fluxes in the Danube River Basin with SWAT." *Science of The Total Environment* 599 (2017): 992-1012.

Wagner, A. (2009). Literature study on the correction of precipitation measurements. FutMon C1-Met-29 (BY), Bavarian State Institute of Forestry, Freising, Germany.

Waidler, D., White, M., Steglich, E., Wang, S., Williams, J., Jones, C. A., & Srinivasan, R. (2011). Conservation practice modeling guide for SWAT and APEX. Texas Water Resources Institute.

Winchell, M., Srinivasan, R., Di Luzio, M., & Arnold, J. (2007). ArcSWAT interface for SWAT 2005. User's Guide, Blackland Research Center, Texas Agricultural Experiment Station, Temple.



11. APPENDIX A - SWAT DATA SOURCE

	Item	Source	Resolution / scale	Comments
Watershed delineation	DEM	DORIS, 2017	0.5/1/10 m	3 DEM available with different resolutions
	River network	DORIS, 2017	catchments 1-10-100 km ²	3 maps with different net resolution
	Water use and transfer locations	DORIS, 2017	26 water withdrawal points	DATA NOT USED
	Lake/reservoir map	DORIS, 2017	ponds > 15 m ²	
	Gauge stations locations	DORIS, 2017	5 points	
	Point source locations	DORIS, 2017	13 municipal WWTPs outlets	
HRU delineation	Land cover map	CORINE Land Cover 2012	The smallest polygon ~100 ha	Principal input data for land cover map. Needed reclassification to SWAT classes
		BMLFUW, 2019	field scale	Improvement of land cover map in agricultural areas
	Soil map	SoilGrids, 2019	250 m raster	Soil textural composition and organic matter content for 7 soil depths
Weather data definition	Precipitation data	HDLO, 2017	15 stations	Daily data
	Temperature data		15 stations	Hourly data preprocessed to get daily maxima and minima
	Wind speed data	ZAMG (Centre for Meteorology and Geodynamics)	1 station (+8 stations outside of catchment)	DATA NOT USED
	Relative humidity data		1 station (+8 stations outside of catchment)	DATA NOT USED
	Solar radiation data		1 station (+8 stations outside of catchment)	DATA NOT USED
Land management	Crop structure	BMLFUW, 2019		Data from several years needed in order to define crop rotations
	Mineral fertilisers	Expert opinion		Required to define fertiliser rates in management schedules
	Livestock / manure	Expert opinion		Required to define manure rates in management schedules
	Other practices (tillage)	Expert opinion		Required for definition of management schedules
	BMPs	Expert opinion	5 small retention basins 3 cross section widening	To be included in NSWRMs implementation step



Water management	Reservoirs	DORIS, 2017	Data for each object	Morphometric parameters, outflow release rules
	Fish ponds	DORIS, 2017	Data for each object	Water uptake, water discharge
	Irrigation	DORIS, 2017	Data for each object	DATA NOT USED
	Water withdrawals	DORIS, 2017	Data for each object	Amount (yearly), source
	Wastewater treatment plants	DORIS, 2017	Equivalent inhabitants, treatments, 2016 data for validation	Loads will be computed based on equivalent inhabitants and loads generation formulations
Groundwater	Hydrogeology maps	DORIS, 2017	5 m isolines	DATA NOT USED
	Ground water monitoring	DORIS, 2017	16 measuring points	DATA NOT USED
Channel	Channel cross-sections	BOKU (University of Natural resources and Life sciences Vienna)	11000 DEM extracted cross sections	Details in Hauer et al., 2015
Soil properties	Soil physical parameters	Literature	Hydraulic conductivity, soil water holding capacity	Pedotransfer functions used
	Soil chemical parameters	Literature	-	DATA NOT USED
pheric deposition	N and P deposition data	Literature	-	No direct measures

Data sources:

LODUWAW, 2017. Bi-weekly water chemistry analysis for 5 gauges. Land Oberösterreich, Direktion Umwelt und Wasserwirtschaft, Abteilung Wasserwirtschaft, Linz

DORIS, 2017. 10m resolution DEM. Digitales Oberösterreichisches Raum-Informationssystem, Linz. Accessed from <https://www.doris.at>

HDLO, 2017. Daily precipitation, maximum/minimum temperatures for 13 weather stations; Daily discharge for 5 gauging stations. Hydrographischer Dienst des Landes Oberösterreich, Linz

GBA, 2019. Geologische Bundesanstalt, Bundesministerium für Bildung, Wissenschaft und Forschung, Wien. Accessed from <https://www.geologie.ac.at>

BMLFUW, 2019. Integriertes Verwaltungs- und Kontrollsystem, Bundesministerium für Land- und Forstwirtschaft, Umwelt und Wasserwirtschaft, Wien. Accessed from www.data.gv.at



12. APPENDIX B- SWAT CALIBRATION RESULTS

Gauging station name	SWAT corresponding subcatchment outlet	Upstream subcatchment
Freistadt	22	1,2,3,4,10,11,16,17,22
Weitersfelden	37	5,6,7,8,13,14,19,20,26,31,37
Kefermarkt	51	9,15,18,21,23,24,25,28,29,32,33,34,35,36,39,40,41,42,43,44,51
Pfahnmule	84	12,27,30,38,45,46,47,48,52,53,54,57,58,60,61,62,63,64,65,66,67,72,73,77,78,84
Shwertberg	103	49,50,55,56,59,68,69,70,71,74,75,76,79,80,81,82,83,85,86,87,88,89,90,91,92,93,94,95,96,97,98,99,100,101,102,103

FLOW Parameters	Gauge number				
	22	37	51	84	94
1:R_CN2.mgt	0.0455	-0.171	-0.1845	-0.1673	-0.1627
2:V_GW_DELAY.gw	132.2912	126.1022	33.6877	101.5887	48.3393
3:V_ALPHA_BF_D.gw	0.1288	0.0921	0.0731	0.0946	0.0897
4:V_ALPHA_BF.gw	0.2093	0.1106	0.0968	0.0703	0.1005
5:V_GWQMN.gw	36.4133	180.5634	310.0715	397.403	68.4921
6:V_GW_REVAP.gw	0.1046	0.0451	0.056	0.1519	0.0795
7:V_REVAPMN.gw	738.1386	698.2445	769.8383	837.2249	698.3586
8:V_RCHRG_DP.gw	0.0336	0.0012	0.0195	0.0476	0.0214
9:R_SOL_K(..).sol	-0.1761	0.2163	-0.1835	-0.0897	-0.0468
10:R_SOL_AWC(..).sol	-0.1596	-0.0655	-0.0067	0.1759	-0.0385
11:R_SOL_BD(..).sol	0.182	0.1393	-0.0274	-0.0535	0.1036
12:R_SLSUBBSN.hru	0.0402	-0.0173	-0.0741	-0.0777	0.1235
13:V_ESCO.hru	0.9584	0.9898	0.607	0.9196	0.7117
14:V_EPCO.hru	0.1751	0.5705	0.5394	0.5426	0.9016
15:R_OV_N.hru	-0.1695	0.1136	0.0395	-0.1708	0.2111
16:V_CH_N2.rte	0.2737	0.2635	0.27	0.2836	0.2506
17:V_SUB_SFTMP(..).sno	0.9291	0.0102	0.4141	-2.5814	0.4723
18:V_SUB_SMTMP(..).sno	0.3373	3.1313	3.2507	0.2889	-0.9532
19:V_SUB_SMFMX(..).sno	3.0114	4.2357	2.9955	1.8779	2.1691
20:V_SUB_SMFMN(..).sno	2.0731	3.1595	2.5993	3.3146	2.701
21:V_SUB_TIMP(..).sno	0.2619	0.5955	0.9571	0.9934	0.8609
22:V_PLAPS.sub	-226.115	-581.317	-607.056	699.7543	-203.768
23:V_NDTARG.pnd	14.0673	11.3807	23.1566	26.1713	6.1073
24:V_PND_K.pnd	0.6756	2.2718	0.3258	2.6977	2.9059
25:R_PND_FR.pnd	-0.1816	-0.2742	-0.2352	-0.022	0.1321
26:R_SOL_ZMX.sol	879.6675	643.5	1084.282	582.3113	1589.278
27:R_SOL_ZMX.sol	447.097	867.6611	696.4084	762.0895	398.7004

NOTE: V: replace; R: relative change



FLOW and SEDIMENT parameters	Calibrated values	Parameters ranges	
		Lower	Upper
1:R__CN2.mgt	0.0048	-0.06224	0.013367
2:R__GW_DELAY.gw	0.4598	0.017823	0.339317
3:R__GWQMN.gw	0.0481	-0.20245	0.126414
4:R__REVAPMN.gw	0.3753	0.219546	0.44044
5:R__RCHRG_DP.gw	-0.0663	-0.19841	0.05045
6:R__SOL_K(..).sol	0.1868	0.150442	0.3243
7:R__SOL_BD(..).sol	0.1329	0.056362	0.152136
8:R__SLSUBBSN.hru	-0.062	-0.04961	0.039047
9:R__ESCO.hru	0.0699	-0.29977	0.017142
10:R__OV_N.hru	0.0199	0.005158	0.101446
11:R__CH_N2.rte	-0.1857	-0.25393	-0.12063
12:R__PLAPS.sub	0.0481	0.075336	0.308026
13:R__PND_K.pnd	-0.1884	-0.22231	-0.07195
14:V__SURLAG.bsn	9.6265	9.381886	14.06746
15:V__ADJ_PKR.bsn	3.5103	0.789785	3.275993
16:V__SPEXP.bsn	1.3283	-0.05598	0.181379
17:V__PND_NSED.pnd	2273.0674	1995.574	3042.065
18:V__PND_D50.pnd	1932.9056	1028.51	3086.708
19:R__CH_W2.rte	0.0879	-0.15388	0.148755
20:V__USLE_C{..}.plant.dat	0.0605	-0.00099	0.049026
21:V__USLE_C{..}.plant.dat	0.0047	0.108961	0.155041
22:V__USLE_C{..}.plant.dat	0.0468	-0.02354	0.04189
23:V__USLE_C{..}.plant.dat	0.0345	0.178889	0.245809
24:V__USLE_C{..}.plant.dat	0.0775	0.033583	0.100781
25:V__PRF_BSN.bsn	1.4345	1.194381	1.521635

NOTE: V: replace; R: relative change